Review

Irena Ban, Janja Stergar* and Uroš Maver*

NiCu magnetic nanoparticles: review of synthesis methods, surface functionalization approaches, and biomedical applications

https://doi.org/10.1515/ntrev-2017-0193
Received August 9, 2017; accepted December 12, 2017; previously published online January 10, 2018

Abstract: Magnetic nanoparticles (MNPs) have attracted extensive interest in recent years because of their unique magnetic, electronic, catalytical, optical, and chemical properties. Lately, research on bimetallic MNPs based on nickel and copper (NiCu MNPs) gained momentum owing to their desired properties for use in biomedicine, such as their chemical stability, biocompatibility, and highly tunable magnetic properties by means of synthesis parameter tuning. The general interest of using NiCu MNPs in biomedical applications is still low, although it is steadily increasing as can be deduced from the number of related publications in the last years. When exposed to an alternating magnetic field (AMF), superparamagnetic particles (such as NiCu MNPs) generate heat by relaxation losses. Consequently, magnetic hyperthermia in cancer treatment seems to be their most promising application in medicine, although others are emerging as well, such as their use to guide potent drugs to the targeted site or to prolong their localization at a desired site in the body. This review is the first, to the best of our knowledge, that covers the available knowledge related to the preparation of NiCu MNPs using different methods, their resulting properties, and the already developed functionalization methods and that discusses everything mentioned in relation to their possible applicability in biomedicine.

***Corresponding authors: Janja Stergar,** Faculty of Medicine, Institute of Biomedical Sciences, University of Maribor, Taborska Ulica 8, SI-2000 Maribor, Slovenia, e-mail: janja.stergar@um.si; and Faculty of Chemistry and Chemical Engineering, Laboratory of Inorganic Chemistry, University of Maribor, Smetanova Ulica 17, SI-2000 Maribor, Slovenia; and **Uroš Maver**, Faculty of Medicine, Institute of Biomedical Sciences, University of Maribor, Taborska Ulica 8, SI-2000 Maribor, Slovenia, e-mail: uros.maver@um.si. http://orcid.org/0000-0002-2237-3786; and Faculty of Medicine, Department of Pharmacology, University of Maribor, Taborska Ulica 8, SI-2000 Maribor, Slovenia
Irena Ban: Faculty of Chemistry and Chemical Engineering, Laboratory of Inorganic Chemistry, University of Maribor, Smetanova Ulica 17, SI-2000 Maribor, Slovenia

Keywords: biomedical applications; magnetic hyperthermia; magnetic nanoparticles; NiCu; synthesis.

Abbreviations: AAO, anodic aluminum oxide; AFM, atomic force microscopy; $Al(acac)_3$, aluminum acetylacetonate; AMF, alternating magnetic field; BET, Brunauer-Emmett-Teller; BPR, ball-to-powder mass ratio; CVD, chemical vapor deposition; DMF, dimethylformamide; DSC, differential scanning calorimetry; EG, ethylene glycol; Fcc, face-centered cubic; FTIR, Fourier transform infrared spectroscopy; GLYMO, 3-(glycidoxypropyl)trimethoxysilane; HCW, hot compressed water; hMSCs, human bone marrow stem cells; MNPs, magnetic nanoparticles; NiCu, nickel and copper; NPs, nanoparticles; PEG, polyethylene glycol; PSE, pulsed-spray evaporation; PVA, poly(vinyl alcohol); PVP, polyvinylpyrrolidone; PVPh, poly(4-vinylphenol); SAR, specific absorption rate; SEM, scanning electron microscopy; T_c, Curie temperature; TEM, transmission electron microscopy; TEOS, tetraethyl orthosilicate; TGA/SDTA, Thermogravimetric analysis/simultaneous differential thermal analysis; VSM, vibrating-sample magnetometer; XPS, X-ray photoelectron spectroscopy; XRD, X-ray powder diffraction

1 Introduction

Magnetic nanoparticles (MNPs) have attracted extensive interest in recent years because of their unique magnetic, electronic, catalytical, optical, and chemical properties. In addition, their extremely small size and large surface area distinguish them from bulk materials [1, 2]. For this reason, they can be part of a wide range of applications related to catalysis, magnetic seals in motors, electronic and mechanical devices, and biomedical applications [3–5]. The last field has seen a significant increase in interest in the last years, especially in magnetic resonance (as contrast agents), in drug delivery (to ensure guidance, tracking, or controlled release), for cell separation (through

specific surface functionalization), and in magnetic hyperthermia [1, 2, 6–10], which is also the focus of this review.

It has been known for a long time that a variety of different diseases can be successfully cured by applying heat. Particularly, the healing power of heat was recognized as a promising method in cancer treatment aside from other well-known established methods of surgery, chemotherapy, and irradiation [11, 12]. This is associated with the findings that cancer growth can be stopped at temperatures higher than approximately 42°C. In order to apply such an approach, we have to overcome two problems; i.e. the temperature increase must be strictly limited only within the target (cancerous) region, leaving all other surrounding healthy tissues unaffected, and the temperature within and outside the target region must be controlled [13].

Magnetic hyperthermia (MH) is one among many techniques used in oncology that is based on heating tissues for therapeutic purposes. MH is usually used as an additive therapy with standard treatments (radiotherapy, for example), and some preliminary studies have shown that the combination of radiation and hyperthermia leads to better results regarding tumor regression [14, 15]. MH can increase the temperature of the tissue because of the use of an alternating magnetic field (AMF) that induces various magnetic loss mechanisms depending on the material properties and the AC magnetic field used [16, 17]. For MH, specific inorganic materials are injected into the body, which is exposed to an AMF. During MH, the energy is absorbed from an AMF and transformed into heat [17] (Figure 1).

The great majority of materials that can be used for MH exhibit a relatively high Curie temperature (T_c) and might overheat the body tissue around the targeted location [18]. Besides, some of these are not suitable materials from the physical point of view, are not biocompatible on their own, and/or have to be covered with a biocompatible coating, as for instance silica or noble metals [18]. In order to eliminate the most disturbing properties of MNPs suitable for hyperthermia, that is, high Curie point and tissue overheating, materials with Curie points in the range of 41–45°C, which cannot cause the overheating of the tissue, are sought for [18].

Among the materials applicable for MH, the iron oxides are the most attractive ones. This is related to their high magnetization, biocompatibility, relatively simple synthesis, and fairly high dissipation [19]. Nevertheless, they also have disadvantages, such as their relatively high T_c [20]. Thus, by application of magnetic iron oxides for MH, not only the target tissue gets efficiently damaged but also the surrounding healthy tissue gets overheated rapidly and damaged if not for an outer temperature control to switch off the magnetic field [21].

Considering the potential drawbacks of other materials, our group focused on bimetallic nickel and copper (NiCu) MNPs, which are particularly attractive and possess all abovementioned positive properties with

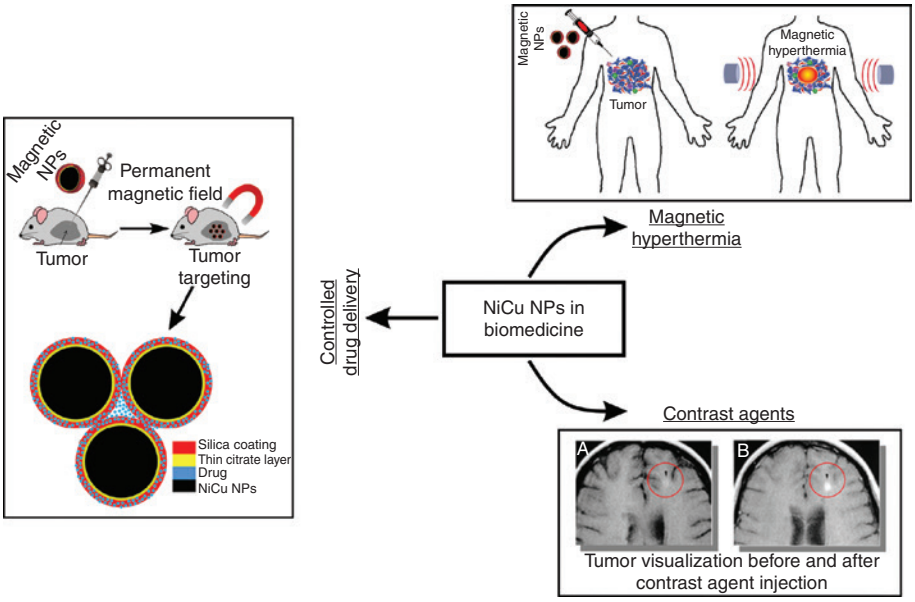

Figure 1: Various applications of MNPs for drug delivery as contrast agent and for magnetic hyperthermia. Left: Incorporation of drugs into coatings on MNPs enables tumor targeting using the magnetic field. Upper right: MNPs can be injected into the tumor, followed by application of an AMF, which results in magnetic hyperthermia. Bottom right: MNPs can be also used as potent and relatively cheap contrast agents.

almost no disadvantages. NiCu MNPs were used before in several application fields, such as in multilayered coatings, contact solar cells, tissue engineering, and biomedical applications [22–25]. NiCu MNPs are chemically stable and biocompatible and exhibit desired magnetic properties, making them interesting for use in biomedicine. They can be synthesized through many different methods, e.g. mechanical milling, hydrothermal-reduction synthesis, microemulsion technique, sol–gel method, polyol reduction process, hydrogen reduction, electrochemical deposition, and plasma evaporation [22, 26–28].

The use of NiCu MNPs in biomedical applications is still a rather new field, but it is attracting an increasing interest as can be deduced from the rising number of related publications published annually in the last decade (Figure 2).

The most promising biomedical application of MNPs seems to be MH in cancer treatment, which is induced by using biocompatible MNPs in the tumor tissue and heating them in an AMF [7, 24, 29–31]. The generated heat depends on the MNPs' chemical composition, resulting in the so-called T_c in the desired range [25]. The desired T_c, leading to selective death of cancer cells upon exposure, lies between 42°C and 46°C [25]. Despite the fact that iron oxides (Fe_3O_4, γ-Fe_2O_3), Fe-doped Au nanoparticles (NPs), and $NiFe_2O_4$ were shown to be very promising for biomedical applications [25], their use in more demanding applications, where the T_c plays an essential role, is inappropriate. Namely, their relatively high T_c leads to overheating and might damage the surrounding healthy tissue as well [32]. Recent findings suggest that NiCu MNPs are also very promising for multimodal cancer therapies, i.e. through combination of MH, and as part of drug delivery systems [33–35].

This review intends to describe different available methods for preparation of NiCu MNPs, their resulting properties, and their optional functionalization and to discuss all mentioned in relation to their applicability in biomedicine.

2 Synthesis of magnetic NiCu MNPs

Magnetic NiCu NPs can be prepared by several physical and chemical methods (Figure 3). Not all methods allow the control of particle size and composition. Considering the increasing importance of environmental sustainability of chemical processes, most of the available preparation methods have limitations also in this regard. Among the most pronounced issues are high operation temperatures, use of harmful organic solvents, use of high-concentration reducing agents, and multistep procedures with (sometimes) low yields [36].

An overview of the available preparation approaches, including the typical characteristics of the formed NiCu structures, is summarized in Table 1.

2.1 Mechanical milling as the method for synthesis

Durivault et al. [37] studied NiCu materials with different compositions synthesized by high-energy ball milling. For the first time, they tested materials for the electrochemical reduction of NO^{3-} in alkaline medium. They prepared a series of $Ni_{100-x}Cu_x$ materials ($0 \le x \le 100$) from elemental Ni and Cu powders using a Spex 8000 laboratory mill (SPEX SamplePrep LLC, USA), wherein the powder mixtures were put into a hardened steel vial with three hardened steel balls. They prepared the powder and steel vial in a glove box under an argon atmosphere. They studied the influences of the milling duration and the ball-to-powder mass ratios (BPR) on the final product characteristics. Using

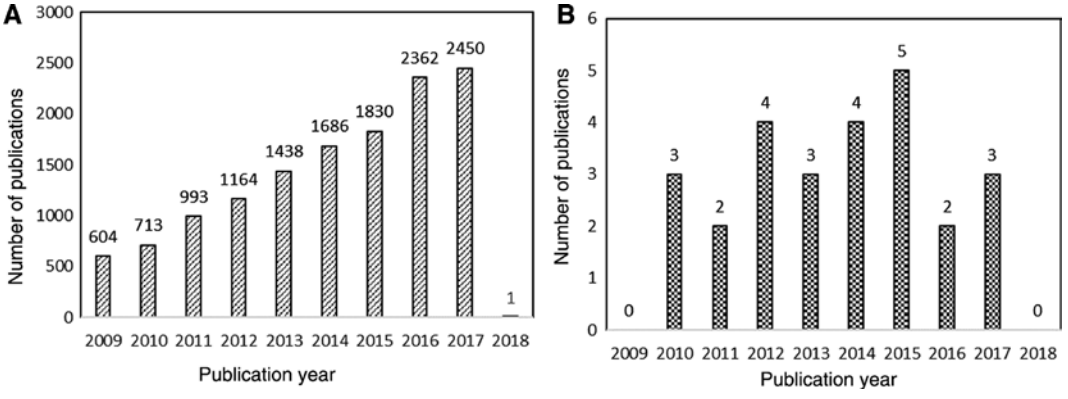

Figure 2: (A) Number of scientific publications contributing to the subject "MNPs AND biomedical applications" and (B) "NiCu NPs AND biomedical applications" by publication year. Search done through *ScienceDirect* on 19 July 2017.

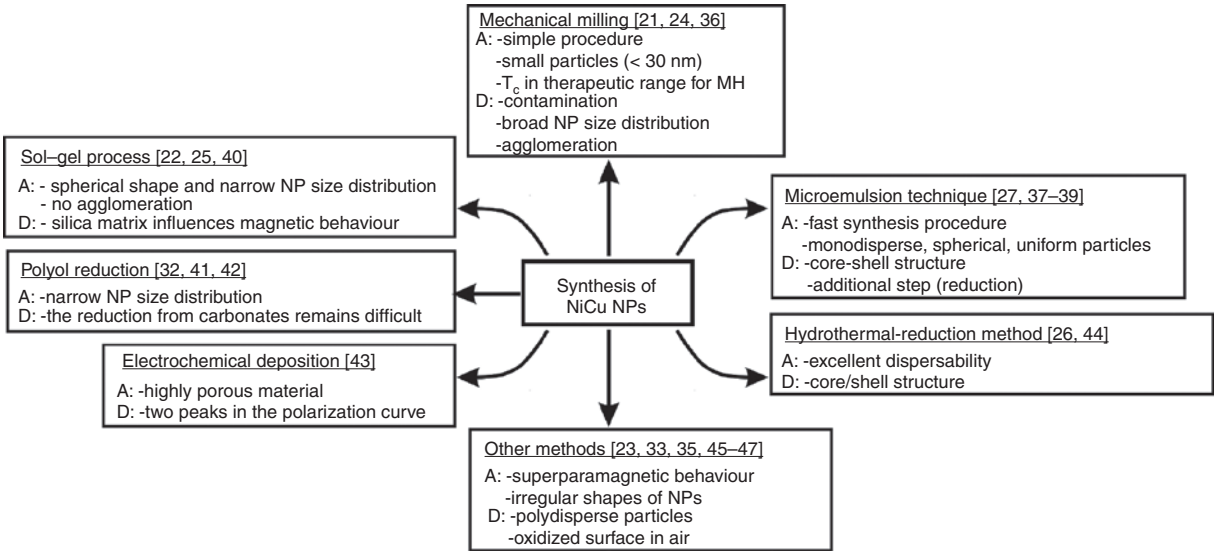

Figure 3: Comparison of the different NiCu MNPs preparation procedures. A→advantages, D→disadvantages, and MH means magnetic hyperthermia.

X-ray powder diffraction (XRD) (Bruker D8 diffractometer, USA) and scanning electron microscopy (SEM) (JEOL JSM6300F, Japan) analysis, they determined the optimal milling conditions for the composition $Ni_{80}Cu_{20}$. They obtained nanocrystalline $Ni_{80}Cu_{20}$ alloys with crystallite size <50 nm, with a good milling yield of >95% and with a very low Fe contamination of <1 atm%. Only the materials with low Fe content could be used for the electrochemical studies. They characterized the prepared NiCu alloy under optimized milling conditions. They clearly proved the catalytic activity of the prepared NPs for nitrate reduction in an alkaline medium [37].

Ban et al. [22] prepared NiCu alloy NPs in the nanometer range by mechanical milling. They ball milled elemental metal powders of Cu and Ni using steel vials in a SPEX 8000M and 8000D mill (SPEX SamplePrep, USA). They loaded and sealed the mixture of powders and vials in a glove box under a nitrogen atmosphere. Optimized milling conditions led to a nanocrystalline $Ni_{72.5}Cu_{27.5}$ alloy with a crystallite size of around 10 nm and a T_c of 45°C. To mitigate the agglomeration of MNPs, they added NaCl during ball milling (NaCl/$Ni_{72.5}Cu_{27.5}$ powder weight ratio was 5:1). They prepared a series of binary powder blends of Ni_xCu_{1-x} ($x = 60$, 70, 72.5, 73, 75, 80) samples after 20 h of ball milling. The size of the particles d_x and the d_{hkl} values were determined by XRD measurements (Bruker AXS, D-5005, USA). After 6 h of ball milling, the preliminary XRD experiments still revealed face-centered cubic (fcc) Cu and fcc Ni phases. Nevertheless, after longer periods (10 and 20 h), they indexed a single fcc phase, which confirmed the formation of a NiCu solid solution of bimetallic NPs. Figure 4 shows the XRD patterns of the binary powder blends of the Ni_xCu_{1-x} (A: $x = 60$, B: $x = 70$, C: $x = 72.5$, D: $x = 73$, E: $x = 75$, F: $x = 80$) samples obtained after 20 h of ball milling under N_2 atmosphere in hardened steel vials [22].

They found that with the increasing content of Cu, the value of d_{111} spacing also increased. The average size of the ball-milled samples was 11 nm (see Table 2).

The plot of magnetization versus the magnetic field of the Ni_xCu_{1-x} alloy particles using a vibrating-sample magnetometer (VSM) (LakeShore 7404VSM, USA) is shown in Figure 5. The hysteresis loops were measured at room temperature under an applied magnetic field of 10 kOe [22]. With increasing content of Ni, the magnetization of the samples increased (the saturation magnetization was between 2 and 50 emu/g). The hysteresis loops of the ball-milled alloy powders showed no remanent magnetization, which indicated the superparamagnetic behavior of the Ni_xCu_{1-x} NPs.

With transmission electron microscopy (TEM) (JEOL 2010F, Japan), they indicated that the NP size distribution was broad with an average particles size of 10 nm (Figure 6). At some location, the particles were partially agglomerated, and they also observed larger grains in the shape of platelets (200 nm long and 5 nm thick) [22].

Ban et al. [22] measured T_c using the modified apparatus thermogravimetric analysis/simultaneous differential thermal analysis (TGA/SDTA) (851^e, Mettler Toledo, USA). The T_c varied with the Ni content; the $Ni_{72.5}Cu_{27.5}$ showed a T_c of around 45°C. Moreover, the abovementioned sample with composition $Ni_{72.5}Cu_{27.5}$ showed a significant heating effect.

Table 1: Overview of the available preparation methods for the synthesis of different NiCu formulations.

Method	Types of materials	MNP size	Feature/comments	Usability	References
Mechanical milling	Nanocrystalline $Ni_{80}Cu_{20}$ alloys	<50	A good milling yield (>95%), a very low Fe contamination (<1 atm%)	As electrode materials for the electrochemical reduction of nitrate and nitrite in alkaline medium	Durivault et al. [37]
	Nanocrystalline $Ni_{72.5}Cu_{27.5}$ alloy	Around 10 nm	T_c of 45°C	Controlled magnetic hyperthermia applications	Ban et al. [22]
	$Ni_{0.5}Cu_{0.5}$ NPs	20 nm	T_c of 44°C, biocompatibility	Hyperthermia	Amrollahi et al. [25]
	NiCu NPs	436 nm	T_c = 46–47°C	Magnetic hyperthermia	Bettge et al. [34]
Microemulsion technique	NiCu alloy NPs	4.49–12 nm	The composition and size of alloy NPs depend on the mole ratio of H_2O to sodium dodecyl sulfate (SDS)	/	Feng and Zhang [28]
	NiCu bimetallic NPs	7–30 nm	Varying composition (Ni_3Cu, NiCu, $NiCu_3$)	/	Ahmed et al. [38]
	$Ni_{49}Cu_{51}$ alloy NPs	4–7 nm	Using oleic acid as stabilizer	/	Wen et al. [39]
	Magnetic Ni_xCu_{1-x} NPs	Around 30 nm	The silica envelope	/	Stergar et al. [40]
Sol–gel method	Magnetic NPs	1–200 nm	The high dispersion	/	Leontyev [41]
	NiCu alloy NPs	Around 16 nm	A narrow particle size distribution	Magnetic hyperthermia	Ferk et al. [26]
Polyol method	NiCu particles	140 nm	A Cu core and a Ni shell	/	Bonet et al. [42]
	NiCu magnetic NPs	50–80 nm	Encapsulation of NiCu NPs by polymer polyethylene glycol (PEG)	Hyperthermia applications	Chatterjee et al. [33]
	NiCu core/shell NPs		Two-step procedure	/	Carroll et al. [43]
Electrochemical deposition	Magnetic alloy nanofilms	/	Surfactants [cetyltrimethylammonium bromide (CTAB), polyoxyethylene(20)stearyl-ether (Brij 78)] were used to control the deposition of nanomaterial	/	Foyet et al. [44]
Hydrothermal reduction	Ultra-fine NiCu bimetallic powders	0.5–2 μm	Dispersion agents (PEG, gelatin) controlled effectively particles size and dispersibility	Microelectronics	Songping et al. [45]
	Ultra-fine NiCu bimetallic powders with core-shell structure	0.5 ± 0.2 μm	Formic acid and glutin were used as hydrothermal-reduction and dispersing agent	Microelectronics	Songping et al. [27]
Hydrogen reduction	NiCu particles	0.2–1 μm	The composition of the alloy could be controlled by changing Ni/Cu molar ratio in starting solution	/	Laurent et al. [20]
	NiCu alloy NPs	5–1000 nm	Applying a magnetic field using a frequency of 440 kHz on the liver resulted in temperature stabilization at 42°C	Magnetic hyperthermia	Kuznetsov et al. [24]
Other methods	NiCu alloy thin films	/	They have shown that high quality thin metallic films can be grown at temperatures that are significantly lower than those needed for the hydrogen reduction route	/	Bahlawane et al. [47]
	NiCu alloy NPs	30–80 nm	Increasing the Ni content led to particle shape changes from ellipsoid to irregular, a significant increase in particle size, and polydispersity	In the field of mask-less printing	Pál et al. [48]

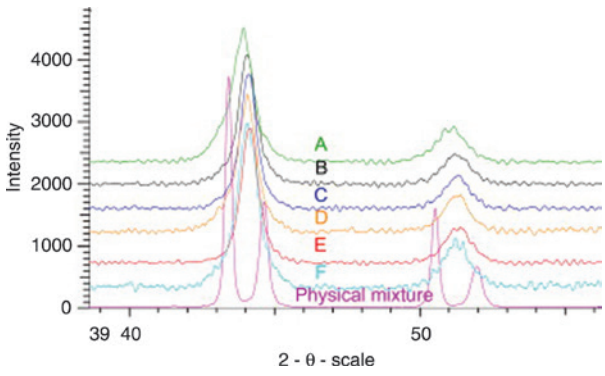

Figure 4: XRD patterns of $Cu_{1-x}Ni_x$ samples with various compositions (A: $x=60$, B: $x=70$, C: $x=72.5$, D: $x=73$, E: $x=75$, and F: $x=80$) and the optimum milling time of 20 h. The patterns are compared with the pattern of physical mixture. Reproduced with permission from Elsevier: *Journal of Magnetism and Magnetic Materials* [22].

Amrollahi et al. [25] studied the cytotoxicity and magnetic characteristics of mechanothermally synthesized NiCu NPs. They milled the mixture of Cu_2O, NiO, and graphite powders in a high-energy planetary ball mill under an argon atmosphere for 30 h; the 10% of graphite acted as a diluent to provide maximum contact area between the reacting particles. They used a vial and balls made of hardened chromium steel. The next step was the heat treatment in a vacuum tube furnace for 1 h at 500°C. After ball milling (30 h) and heat treatment (1 h, 500°C), they obtained single-phase $Ni_{0.5}Cu_{0.5}$ NPs with a narrow size distribution of about 15 nm. Their NPs were highly agglomerated in majority, resulting from experiencing elevated temperatures through heat treatment. They investigated the magnetic properties using a VSM (Meghnatis Daghigh Kavir Co., Iran) based on the results of the hysteresis loop of the milled and heat-treated samples measured as follows: saturation magnetization of 18 emu/g, coercivity of 25 Oe, and magnetic remanence of 2 emu/g. The T_c of the single-phase $Ni_{0.5}Cu_{0.5}$ was 44°C. By analyzing the effect of $Ni_{0.5}Cu_{0.5}$ NPs on proliferation of human bone marrow stem cells (hMSCs), biocompatibility was proven [25].

2.2 Synthesis using the microemulsion technique

Feng and Zhang [28] prepared NiCu NPs using simultaneous reduction of $CuSO_4$ and $NiCl_2$ with hydrazine in a microemulsion of SDS/*n*-butanol/*n*-heptane/water at 70°C. In the microemulsion mixture, they used SDS as the surfactant, *n*-butanol as the cosurfactant, *n*-heptane as the continuous oil phase, and Cu^{2+} and Ni^{2+} precursor solution or hydrazine solution as the dispersed aqueous phase. They established a series of partial phase diagrams at room temperature by locating the demarcation between the microemulsion and non-microemulsion regions of the mentioned systems with different w (w=[water]/[surfactant]). Furthermore, they mixed two stable microemulsions at 70°C. After formation of the NiCu MNPs at 70°C, they separated NPs from microemulsion and analyzed them. TEM analysis (JEOL 2000FXII, Japan) showed typical Ni-Cu NPs with an average diameter of 12 nm, whereas electron diffraction pattern indicated an fcc lattice structure. Also, the XRD analysis (Rigaku D/MAX-2200 X-ray diffractometer, Japan) confirmed an fcc structure of Ni-Cu alloys, which were not completely crystalline. They also found that the particle composition and size control depended on many parameters: the w value, the method of addition, and the mole ratio of Cu^{2+} and Ni^{2+} in the precursor solution. The change of w was in relation with the water droplet size. They found that the difference in the reduction potential was a crucial factor to determine the structure of the particles. A large difference in the reduction potential led to a core-shell structure and a small difference in the alloy composition. With TGA, they indicated that their Ni-Cu nanocomposites or NPs oxidized easily even at room temperature and that the oxidation was completed before reaching 200°C [28].

Ahmed et al. [38] synthesized bimetallic NiCu NPs (1:3, 1:1, and 3:1) using the microemulsion route with CTAB (Spectrochem, 99%, IN, USA) as the surfactant, 1-butanol (Qualigens, 99.5%, USA) as the cosurfactant, and isooctane (Spectrochem, 99%, IN, USA) as the oil

Table 2: Composition, Curie temperature T_c, magnetization M, average particle size from X-ray diffraction d_x, average particle size from magnetization measurements d_M, standard deviation σ, and d_{111} spacing of Cu-Ni materials [22].

Sample	w (atm%)	T_c (°C)	M (emu/g)	d_x (nm)	d_M (nm)	σ (A/m)	d_{111} (Å)
A	$Cu_{40}Ni_{60}$	–	4.4	10	–	–	2.0595
B	$Cu_{30}Ni_{70}$	24	17.5	11	10	0.42	2.0544
C	$Cu_{27.5}Cu_{72.5}$	45	20.7	12	11	0.37	2.0516
D	$Cu_{27}Ni_{73}$	53	13.2	11	10	0.45	2.0520
E	$Cu_{25}Ni_{75}$	137	48.5	11	7	0.23	2.0503
F	$Cu_{20}Ni_{80}$	174	32.9	10	9	0.30	2.0398

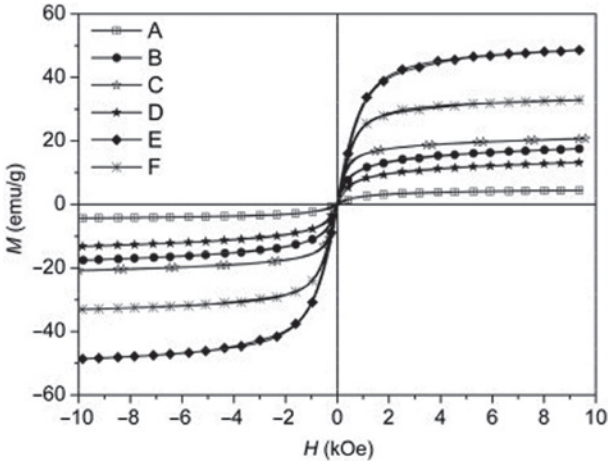

Figure 5: Magnetization versus magnetic field of $Cu_{1-x}Ni_x$ alloy particles, samples (A–F) ball-milled for 20 h. Reproduced with permission from Elsevier: *Journal of Magnetism and Magnetic Materials* [22].

phase. They prepared four different microemulsions with different aqueous phases. Microemulsion I contained $Cu(NO_3)_2 \times 3H_2O$ (0.1 M, CDH, 98%, IND), microemulsion II contained $Ni(NO_3)_2 \times 6H_2O$ (0.1 M, Qualigens, 99%, IN, USA), microemulsion III contained $N_2H_4 \times H_2O$ (20 M, Qualigens, 99%, IN, USA), and microemulsion IV contained NaOH (0.1 M, Qualigens, 97%, IN, USA). They mixed all microemulsions from I to IV and annealed the formed green precipitate in hydrogen atmosphere at 500°C for 5 h, which led to the formation of a monophasic bimetallic NiCu, Ni_3Cu, and $NiCu_3$ alloy black powder. With XRD analysis (Bruker D8 Advance diffractometer, USA), they proved the products based on the fcc cell and that the lattice parameter increased with the increase in Cu content. TEM studies (Technai G2 20, FEI, USA) showed nearly monodispersed, spherical, and uniform NiCu particles with an average size of around 7 nm, whereas particles of Ni_3Cu and $NiCu_3$ agglomerated and were also larger (20–30 nm). Ahmed et al. [38] confirmed that when the concentration of Cu in the nanocrystalline alloys increased, the magnetization decreased. The results obtained with the Brunauer-Emmett-Teller (BET) method showed a decrease in the surface area with the increasing concentration of Cu [38].

Wen et al. [39] synthesized NiCu NPs with the microemulsion method using oleic acid as the surfactant. They prepared a mixture of NaOH (Sinopharm Chemical Reagent Co. Ltd., China), deionized water, and ethanol, later adding oleic acid (Sinopharm Chemical Reagent Co. Ltd., China) and hexane to the mixture. The aqueous solutions of $CuSO_4 \times 5H_2O$ and $NiCl_2 \times 6H_2O$ (both purchased from Sinopharm Chemical Reagent Co. Ltd., China) were added to this, which formed a stable and transparent microemulsion under vigorous stirring. After adding KBH_4 (Sinopharm Chemical Reagent Co. Ltd., China), which was dissolved in deionized water, the solution changed immediately from transparent cyan to black. After the reaction, they disrupted the micelle solution by adding hexane, and NiCu NPs coated with oleic acid were extracted into the oil phase. They annealed the product at 923 K for 0.5 h in an argon atmosphere and compared the resulting material before and after annealing. The hysteresis loops were measured at room temperature using VSM (Lake Shore model 7307, USA) under an AMF; in both cases (as-synthesized and annealed sample), a hysteresis was observed. The saturation magnetization and coercivity increased after annealing. The XRD analysis (Rigaku Corporation D/max 2550 X-ray diffractometer, Japan) indicated that the as-synthesized NPs were amorphous, whereas the crystallinity increased after annealing. With the TEM analysis (JEOL JEM-1200EX, Japan), they observed a uniform particle distribution for the as-synthesized NPs with an average size of 4–7 nm without any aggregation. TGA/differential scanning calorimetry (DSC) (NETZSCH (STA409PC), NL, USA) analysis confirmed the thermal stability and the crystallization behavior. The weight loss for NiCu NPs coated with oleic acid occurred from 572.2 to 651.9 K, which

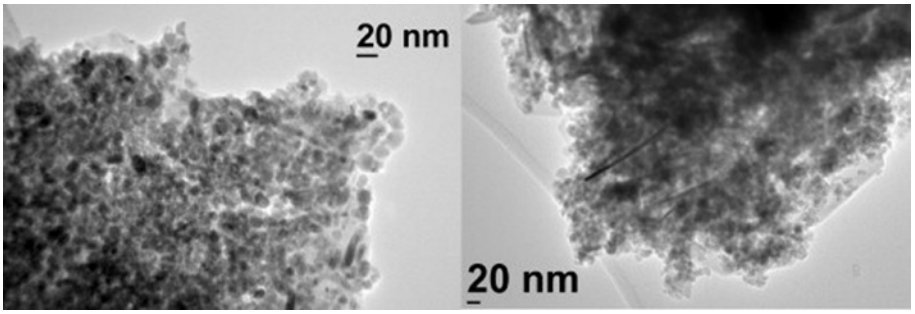

Figure 6: TEM micrograph of mechanically alloyed $Cu_{27.5}Ni_{72.5}$ particles (sample C). Reproduced with permission from Elsevier: *Journal of Magnetism and Magnetic Materials* [22].

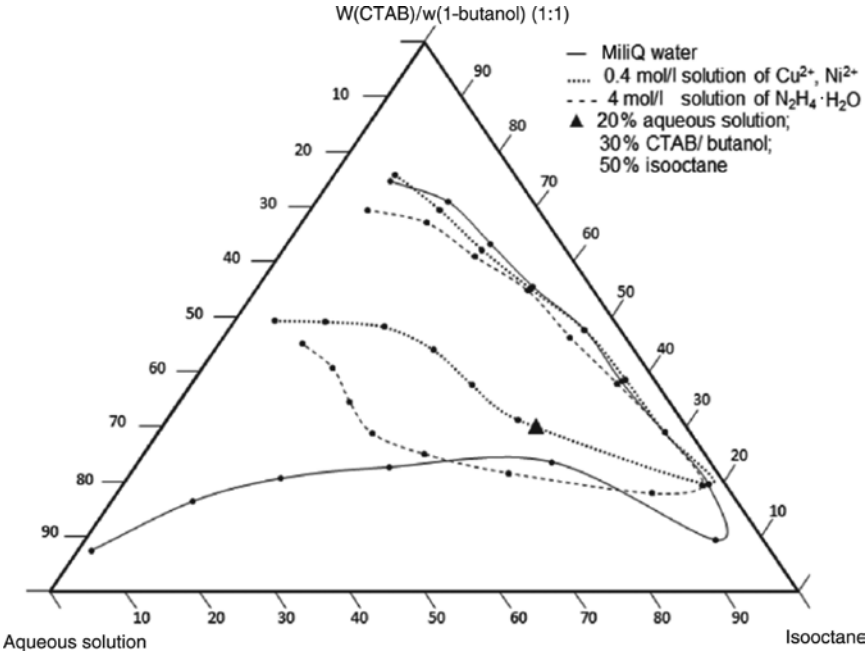

Figure 7: Region of microemulsion stability is indicated as a function of the concentrations of reagents in the solution. Composition of the reverse micelles used to synthesize the particles is marked with ▲. Reproduced with permission from IEEE: *Transactions on Magnetism* [40].

corresponds to the evaporation and decomposition of the oleic acid and the other organic reagents [39].

Stergar et al. [40] synthesized magnetic Ni_xCu_{1-x} NPs with a water-in-oil (w/o) microemulsion using water/CTAB and *n*-butanol/isooctane (all Sigma-Aldrich, Germany), in which the reduction of $NiCl_2$ and $CuCl_2$ (both from Sigma-Aldrich, Germany) was induced through hydrazine and NaOH (Sigma-Aldrich, Germany). Two microemulsions were used: microemulsion A contained different concentrations of metal ions (Cu^{2+} and Ni^{2+}), while microemulsion B contained hydrazine and sodium hydroxide. Figure 7 shows the phase diagram of water/CTAB and *n*-butanol/isooctane system, which was used as a starting point for the preparation of the microemulsions. They used the titration method to select a proper compositional range that would form a microemulsion in the water/CTAB and *n*-butanol/isooctane system (composition used to synthesize the particles is marked) [40].

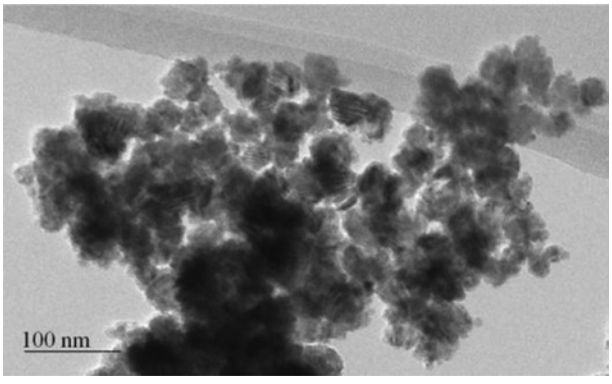

Figure 8: TEM image of a typical $Cu_{1-x}Ni_x$ alloy particles obtained in a microemulsion. Reproduced with permission from IEEE: *Transactions on Magnetism* [40].

Microemulsions A and B were mixed for 20 min at 60°C in an air atmosphere. Then, the MNPs were collected, washed, and subjected for further characterization. The next step was homogenization in a tube furnace, and NPs were coated with silica to prevent agglomeration during heat treatment. TEM analysis (JEOL 2010F, Japan) of as-prepared MNPs showed partially agglomerated MNPs with an average size of around 30 nm (Figure 8); the XRD patterns (measured using Bruker D5005 diffractometer, USA) confirmed the fcc solid-solution phase of Ni_xCu_{1-x} [40].

The measured T_c of the as-prepared samples were close to that of pure Ni, which indicated a core-shell structure, where the Ni shell determined the final T_c. Ni and Cu have different reduction potentials, so first, the Cu was nucleated and then also Ni, which was deposited on Cu. Therefore, MNPs were homogenized in a reducing atmosphere in tube furnace at 500°C in order to reach a homogenous distribution of both constitutive elements, forming the solid solution with a T_c according to the nominal composition. T_c was measured with a modified TGA/SDTA method (Mettler Toledo 851e, USA). In order to prevent agglomeration during heat treatment, NPs were

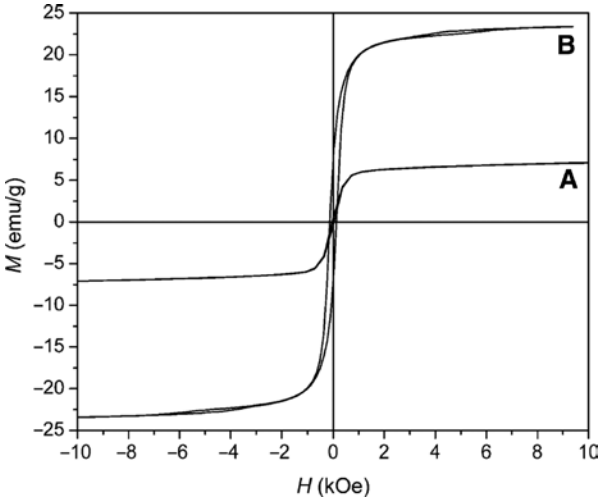

Figure 9: Coating of particles affects their magnetic properties. Magnetization measurement is therefore a good way to determine the influence of the prepared coating. (A) Magnetization versus magnetic field for the silica-coated particles and (B) "as prepared" particles. Reproduced with permission from IEEE: *Transactions on Magnetism* [40].

coated with silica in an ultrasonic bath for 24 h at 60°C. Spherical particles coated with silica were then homogenized in a tube furnace at 900°C. No agglomeration was observed during this step. The T_c for both the uncoated and coated homogenized NPs were the same. The sample with composition $Ni_{72.5}Cu_{27.5}$ reached T_c of 65°C. In Figure 9 we can see the magnetization of the uncoated and coated samples, which were 22 and 7 emu/g, respectively [40].

The silica coating influenced the magnetization but could be thinned and/or removed with NaOH. It has been established that the silica coating prevented agglomeration of the alloy NPs during thermal treatment and that the MNPs were therefore isolated with a biocompatible layer [40].

2.3 Synthesis using the sol–gel process

Leontyev [41] synthesized NPs from pure Ni and NiCu solid solutions with the sol–gel method. First, the author prepared an ultradispersed powder mixture of Cu and Ni hydroxides with a molar ratio of Ni/Cu = 87.5/12.5. The author separated the formed precipitate from the solution by filtration and dried the precipitate at 80°C. Then he loaded the precipitate hydroxide into a quartz crucible and heated it to 400–600°C in a tube furnace under nitrogen for 30 min. Metal powders were prepared using hydrogen reduction at different temperatures. The NPs in the powders were polydispersed (1–200 nm) and almost spherical. The temperature range of the magnetization increased with decreasing NP size with a diameter below 100 nm, which was explained through the powder polydispersity. The smallest particles provided high magnetization at room temperature and a high value of T_c and vice versa for larger particles [41].

Ferk et al. [26] synthesized NiCu MNPs with a narrow size distribution by reducing a Ni and Cu oxide mixture in a silica matrix, using the sol–gel method. For this purpose, they dissolved $Ni(NO_3)_2 \times 6H_2O$ (Merck, Germany), $Cu(NO_3)_2 \times 3H_2O$ (Prolabo, France), and citric acid (Sigma-Aldrich, Germany) in deionized water, and after vigorous stirring, they added absolute ethanol and tetraethyl orthosilicate (TEOS) (Sigma-Aldrich, Germany) to the solution. They stirred vigorously until a two-phase system was converted into a single homogenous phase solution. They dried the sol for 3 days at room temperature. Afterward, they calcinated the gel in air at 500°C for 24 h. They prepared the Ni and Cu oxides in the SiO_2 matrix, which were reduced in H_2/ Ar atmosphere for 24 h at 850°C. The final product was $Ni_{1-x}Cu_x$ NPs in the silica (SiO_2) matrix [26]. They removed the silica matrix with an etching solution (NaOH/3 wt.% hydrazine hydrate) under stirring for several hours in an argon atmosphere. They finally dispersed the produced NiCu MNPs in absolute ethanol. They found that the addition of hydrazine hydrate to the NaOH solution was a key factor to remove the silica matrix. With XRD (Bruker D5005 diffractometer, USA) and Fourier transform infrared spectroscopy (FTIR) (Shimadzu IRAfinnity-1, Japan) analyses, they confirmed the presence of NiCu NPs without the silica matrix and without oxides as the final product. They conducted the final examination by using TEM analysis (JEOL 2010F, Japan). They compared the TEM images of the $Ni_{67.5}Cu_{32.5}$ NPs before and after etching for 24 h, and the images showed that the SiO_2 matrix was washed away. Moreover, only spherical NPs of $Ni_{67.5}Cu_{32.5}$ with a narrow size distribution remained. They measured T_c with a modified TGA (Mettler Toledo 851e, USA): for the $Ni_{67.5}Cu_{32.5}$, they determined T_c of 65°C. They also performed calorimetric measurements in an AMF with a field strength of 4.2 kA/m and using four different frequencies [26]. They established that the self-heating temperature curves converged to the limiting temperature and that the difference between steady-state temperatures decreased, although the frequency of the field increased. This was the first reported method that promised the synthesis of superparamagnetic NiCu particles with a narrow size distribution, allowing control of T_c [26].

Ferk et al. [23] synthesized NiCu alloy MNPs with a range of T_c from 51°C to 63°C by the reduction of intimately mixed Ni and Cu oxides in a silica matrix using the sol–gel method with some minor changes. The procedure of the

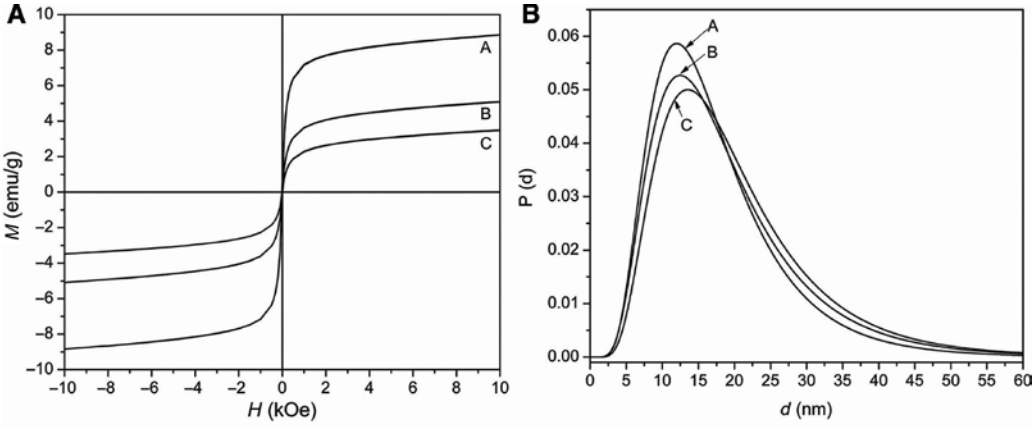

Figure 10: Magnetization properties are often related also to the grain size of respective particles. (A) Magnetization of synthesized NPs at 293 K (A: $Ni_{67.5}Cu_{32.5}$, B: $Ni_{62.5}Cu_{37.5}$, and C: $Ni_{60}Cu_{40}$) versus the magnetic field and (B) corresponding grain size distribution obtained from the magnetic measurement. Reproduced with permission from Elsevier: *Journal of Alloys and Compounds* [23].

synthesis was the same as the previous one, up to the point when the green solid gel product was formed [26]. Then they calcinated the formed gel in air at 800°C for 6 h. They got a solid solution of Cu_2O-NiO in a SiO_2 matrix and reduced this product in a H_2/Ar atmosphere for 6 h at 850°C. They removed the silica matrix as reported previously [26]. They found that the heat treatment in air at a higher temperature of 800°C brought about the formation of the solid solution Cu_2O-NiO, and the fcc structure of the Cu oxide Cu_2O prevailed, which is compatible with the NiO structure. The XRD (Bruker D5005 diffractometer, USA) results indicated the formation of an oxide solution with an average crystallite size of 5 nm. The next step was the homogenization and growth of NiCu alloy MNPs in silica matrix, which inhibited agglomeration and coarsening.

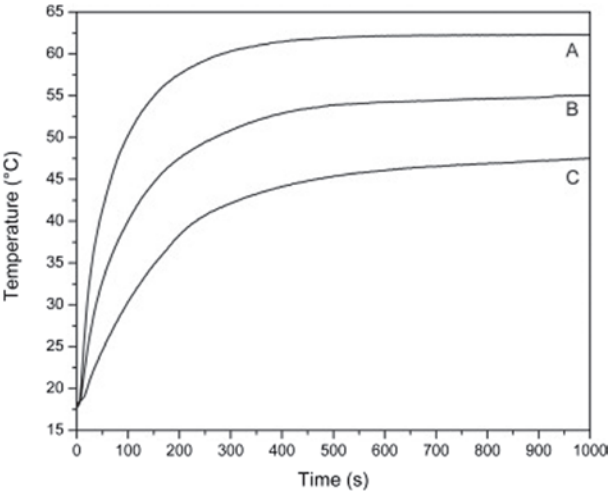

Figure 11: The calorimetric measurements of samples A, B, and C at a magnetic field of 29.4 kA/m and a frequency of 100 kHz. Reproduced with permission from Elsevier: *Journal of Alloys and Compounds* [23].

With the diffraction analysis, they proved the single-phase composition of the target alloy compounds and that there were no secondary phases. The MNPs in silica matrix were well crystallized with an average size between 17 and 19 nm. TEM analysis (JEOL 2010F, Japan) showed spherical grains/NPs, which were not agglomerated. The measured T_c increased with increasing Ni content in the samples and were in the range from 51°C to 63°C. The magnetizations of the bare $Ni_{67.5}Cu_{32.5}$ (A), $Ni_{62.5}Cu_{37.5}$ (B), and $Ni_{60}Cu_{40}$ (C) NPs were measured (Lake Shore 7307 vibrating-sample magnetometer, USA) with respect to the magnetic field at 293 K (Figure 10). The measured NPs had a similar size, so that the size effect on the magnetization can be neglected and the saturation magnetization difference between the particles of various compositions must depend on the fraction of Ni atoms in the $Ni_{1-x}Cu_x$ alloy [23].

The specific absorption rate (SAR) of the sample in an AMF was measured calorimetrically in an AC magnetic field at a frequency of 100 kHz and a magnetic field of 29.4 kA/m. The initial heating rates for the sample were obtained from the heating curves shown in Figure 11 and used to determine the SAR [23]. The SAR values increased with increasing Ni content in the samples.

These results indicated that the synthesis of NiCu alloy MNPs with various T_c using a reduction of intimately mixed Ni-Cu oxides in a silica matrix at 850°C attained by a sol–gel method is a convenient method for synthesizing magnetic particles with a controlled T_c [23].

2.4 Synthesis through polyol reduction method

Bonet et al. [42] synthesized bimetallic NiCu particles from either suspensions of $NiCO_3$ (Outokumpu, FIN) and

$CuCO_3$ (Prolabo, France) or solutions of $Ni(NO_3)_2$ (Merck, Germany) and $Cu(NO_3)_2$ (Prolabo, France) in ethylene glycol (EG) (Prolabo, France), which acted both as solvent and reducing agent. They mixed Ni and Cu compounds to produce bimetallic $Ni_{80}Cu_{20}$ particles with EG at room temperature under magnetic agitation. Then they heated the system because carbonate compounds are not insoluble in EG at room temperature. At the end of reaction time, they separated the solids from the liquid by centrifugation, washed with acetone, and dried the product in air. They found that the reduction from the carbonates was rather difficult and that the increase in time did not compensate for the temperature effect. After 39 h of the reaction at 140°C, a Cu-rich NiCu solid solution and a Ni-rich NiCu solution were obtained. They confirmed these results using XRD analysis (Philips PW 1710 diffractometer, Belgium). The final product (black powder) also contained a green solid and was shown to include undissolved reactants even after 39 h. They tried also with higher temperature, 190°C, but the XRD patterns also showed three double peaks. An increase in temperature aided dissolution of the reactants but did not contribute to the formation of a single solid solution. The SEM analysis (Philips XL FEG30 apparatus, Belgium) showed small quasi-spherical particles and big particles with clear evidence of sintering. They also tried to prevent sintering with a protecting agent, polyvinylpyrrolidone (PVP) (Prolabo, France), but they got also two distinct phases. Then they studied the reaction with the nitrate salts whose solubility is higher in glycols. The reaction extended at 196°C for 4 h. TEM analysis (JEOL 2010, Japan) showed bimetallic polyhedral NiCu particles with an average size of 140 nm, a narrow distribution, and almost no sintering. XRD confirmed a Cu core and a Ni shell of the NPs. They explained the mechanism of formation of bimetallic Ni-Cu particles with a Cu core and a Ni shell. Cu(II) species reduced to Cu(0) at a temperature lower than that required to reduce Ni(II) to Ni(0) [42].

Chatterjee et al. [33] also synthesized NiCu NPs by a polyol reduction method. They mixed metallic precursors in EG with NaOH (both Sigma-Aldrich, USA) and heated the mixture to 195°C. The reaction extended under the reflux. After a few hours, they precipitated the metal alloy particles from the solution, centrifuged, washed with ethanol, and dried the product in air at 50°C. They prepared three different compositions, $Ni_{30}Cu_{70}$, $Ni_{70}Cu_{30}$, and $Ni_{40}Cu_{60}$. The resulting particles had a uniform shape and an average size of 50–80 nm (measured by TEM, JEOL 2010, Japan). The $Ni_{70}Cu_{30}$ NPs exhibited a T_c of ~77°C, a saturation magnetization of ~45 emu/g (measured by Quantum Design MPMS 5 SQUID, USA), and a superparamagnetic behavior [33].

Carroll et al. [43] prepared NPs with different Ni/Cu (or Cu/Ni) core/shell compositions using the polyol method. A series of experiments, in which hydrated Cu chloride, hydrated Ni chloride, and sodium hydroxide (all Fished, USA) were dissolved in EG (Acros Organics, USA) and rapidly heated to the boiling point (~165°C), was performed. They ascertained that the prepared solution boiled at the mentioned temperature, and after the removal of the water with hydration from the solution, the boiling point increased to 175°C. This 10°C difference was sufficient to separate the formation of elemental Cu under reflux conditions from the formation of elemental Ni under distillation conditions. They concluded that the temperature, as well as the absence of water, played an important role in the actual reaction mechanism to prepare Ni shell/Cu core NPs. They prepared the Ni core/Cu shell NPs in a two-step process. In the first step, they distilled a Ni chloride solution until Ni NPs formed. After completion of the reaction, they added a Cu chloride solution and then heated at reflux conditions leading to the formation of Cu shells on the Ni NPs. TEM analysis (JEOL JEM-3010, Japan) showed the formation of the Cu/Ni and Ni/Cu core-shell NPs. With XRD analysis (Panalytical X'Pert Pro powder diffractometer, UK), they confirmed the formation of Cu/Ni and Ni/Cu core-shell NPs, and they compared the results with elemental Ni and Cu. The magnetization measurements (Lakeshore model 7300 vibrating sample magnetometer, USA) showed hysteresis loops. The saturation magnetization of the Cu/Ni NPs ($Ni_{36}Cu_{64}$) was 18.15 emu/g and for Ni/Cu NPs ($Ni_{38}Cu_{62}$) was 19.65 emu/g. With these results, they identified a new and simple procedure for separating the formation of elemental Cu and Ni in a polyol-type procedure [43].

2.5 Synthesis using electrochemical deposition

Foyet et al. [44] developed a double template electrochemical method to prepare NiCo and NiCu magnetic nanofilms. They prepared anodic aluminum oxide (AAO) by a modified two-step anodization. The first plating mixture consisted of 60 wt.% Brij78 and 40 wt.% of aqueous solution containing $CuSO_4$, $NiSO_4$, and H_3BO_3 (all Acros Organics, USA). The second liquid crystal template consisted of 50 wt.% of CTAB and 50 wt.% of aqueous solution containing $CuSO_4$, $NiSO_4$, and H_3BO_3 (all Acros Organics, USA). They used a 273A potentiostat/galvanostat model (Princeton Applied Research, USA) with two electrodes consisting of Al_2O_3/Al and a platinum foil for all electrochemical depositions. The average height of the samples was 300 nm in the case

of the NiCu film, while the surface-to-volume ratio was very high in the prepared NPs. Inclusion of a surfactant during synthesis significantly increased the porosity of the NiCu magnetic nanofilms. Atomic force microscopy (AFM) (TopoMetrx TMX 2010 Discoverer) results showed that the thickness of the porous alumina template was less than 60 nm. The topography appeared as if the pores of the membrane were filled in a homogenous manner by metal particles. The average height of the samples was 300 nm for NiCu film, and the surface-to-volume ratio was very high in NPs. To reduce the size of particles and increase the specific area of the film, they combined the hexagonal phase of the liquid crystals (Brij78 and CTAB) with the AAO as template for deposition. When they prepared this material in the presence of Brij78 liquid crystal mixture, the samples had double substructures. One was due to the pore of the aluminum oxide membrane, and the second subdivision was caused by the columns of the liquid crystal that divided the nanorods into many small particles. In the case of the CTAB liquid crystal structure, the material was highly porous, and many small particles could be observed in each pore of the AAO. They found that the porosity of NiCu magnetic nanofilms increased significantly when these materials were prepared in the presence of the surfactant. Both surfactants (Brij78 and CTAB) gave nanostructured films with two repeat distances. The double template process showed the increase of specific surface area of the film and also the improvement of the physical and chemical properties of these nanomaterials. The polarization behavior of NiCu NPs exhibited two anodic peaks that can be attributed to the successive oxidation of Ni and Cu. The corrosion potential of the alloys seemed to depend on the size of NPs; films deposited in the presence of CTAB and AAO show a smaller particle size and a more negative corrosion potential compared with the ones deposited directly from solution into AAO [44].

2.6 Synthesis by the hydrothermal reduction method

Songping et al. [45] synthesized ultrafine Ni-rich NiCu bimetallic powders using polyethylene glycol (PEG) and gelatin as protective agents. They mixed $NiSO_4 \times 6H_2O$ and $CuSO_4 \times 5H_2O$ with Na_2CO_3 to obtain solution 1, and they mixed HCOOH and NaOH to obtain solution 2. They mixed the two solutions and heated it in a titanium material autoclave at the temperature of 230°C for 18 h to reduce the Ni-Cu ion to metallic powders. They washed the product with hydrochloric acid and with distilled water and dried it at 60°C in a vacuum drier. They used as-prepared Ni-rich bimetallic powders as the functional material for thick film pastes. The XRD pattern of the NiCu bimetallic powders indicated characteristic peaks for Cu and Ni. They found that in order to prepare fine powders with the chemical reduction method, it was crucial to choose an appropriate dispersion agent. When PEG was employed as a protective agent, flake bimetallic powder particles exhibited an excellent dispersibility, a uniform size (1.8–2.0 μm), and a thickness of 100 nm. Using gelatin resulted in the formation of monodispersed non-agglomerated NiCu polyhedral powder particles with a smooth surface and a diameter of 0.5–0.8 μm. Conductive thick films prepared using the NiCu NPs had a low resistivity and high adhesion strength [45].

Songping et al. [27] synthesized NiCu powders using the hydrothermal reduction method by using formic acid and glutin as the hydrothermal reduction and dispersion agents, respectively. They mixed two solutions in autoclave, the first containing $NiSO_4 \times 6H_2O$, $CuSO_4 \times 5H_2O$, and Na_2CO_3 and the second containing HCOOH and NaOH. They heated the autoclave at 230°C for 20 h to reduce NiCu ions in the solution to a metallic powder. Temperature and reaction time were important factors for synthesizing a NiCu powder. The dispersibility of powders increased by increasing the reaction time. They studied the influence of glutin on the shape and size of the formed NiCu particles. When they used $w_{glutin}/w_{metal} = 20\%$, the size of the quasi-spherical particle was 1.5 ± 0.2 μm, and the agglomeration was terrible. When they used the ratio of $w_{glutin}/w_{metal} = 80\%$, the size of polyhedral particles was 350 ± 50 nm, and their dispersibility was excellent. When they increased the ratio up to 240%, different shapes of particles occurred in the range of 0.1–1.2 μm. They also studied the influence of formic acid on the formed NiCu particles. The size of quasi-spherical particles was in the range of 0.2–1.8 μm, and the agglomeration was highly present when they used a weight ratio of formic acid around 120%. When they used a higher ratio of 200%, the size of particle was 0.5 ± 0.2 μm, and dispersibility was excellent. When they used ratios up to 350%, they got lots of small particles with a diameter of 50 nm. The size of powders decreased with an increasing amount of glutin or formic acid. SEM analysis (Philips XL30deltaDX-4i, Belgium) indicated that the NPs contained a predominantly Cu(core)/Ni(shell) structure [27].

2.7 Use of other methods for synthesis

Bettge et al. [34] synthesized NiCu NPs through the combination of two methods, namely, the melting of a NiCu

mixture and ball milling of the resulting bulk alloy. The mixture had a composition of $Ni_{71}Cu_{29}$. First, they ball milled the mixture for 2 h to obtain a highly homogenous composition over the resulting bulk alloy. Then they heated this mixture up to 1465°C for 3 h under nitrogen to prevent oxidation. After melting, they used a continuous grinding and additional grinding up in a ceramic ball mill for at least 3–7 days to break down the bulk chunk to the desired particle size. They used a wet, acetone-based environment in order to prevent oxidation. The magnetic measurements of the as-produced bulk alloy in a magnetic field of 100 Oe indicated a complete phase transition from ferromagnetic to paramagnetic behavior at 97°C. The coarse sand-grinded powder (particle diameter of <150 μm) showed a T_c of ~72°C, while the fine ball-milled powder (436 nm) showed a T_c ~46–47°C. No remanent magnetic moment at room temperature indicated the superparamagnetic behavior of the Ni-Cu ball milled powder. TEM analysis (JEOL 2010, Japan) confirmed the effectiveness of combined methods to produce alloy particles in large quantities. Nevertheless, monodispersity and distribution uniformity could not be ensured [34].

Sue et al. [36] synthesized Cu and NiCu particles from Cu and Ni formates in hot compressed water (HCW). They prepared $Ni(COOH)_2 \times 2H_2O$ and $Cu(COOH)_2 \times 4H_2O$ (both from Wako Pure Chemicals, Japan) solutions in distilled water by dissolving, with a variable Ni/Cu molar ratio. The reaction was performed in a titan alloy batch reactor in nitrogen atmosphere. They quenched the reactor in a water bath, formic acid decomposed into hydrogen and carbon dioxide, and yields of H_2 and CO_2 increased to 90% at 673 K within 2 s. NiCu NPs formed from their formates owing to hydrogen reduction in HCW. SEM analysis (JEOL JSM-5400LVS, Japan) showed the particles with diameters ranging from 0.2 to 1.0 μm. The XRD patterns (measured by Rigaku RAD-B system with monochrometer, Japan) indicated production of both Ni-rich and Cu-rich crystals. When they raised the Cu concentration in the starting solution, the Cu share of the Ni-rich alloy firstly increased, but a further increase in the molar ratio resulted in a decreased Cu share. Hence, the alloy composition could be controlled by changing the Ni/Cu molar ratio in the starting solution [36].

Kuznetsov et al. [24] prepared NiCu alloy particles by coprecipitation of salts from solution followed by reduction in hydrogen. They coprecipitated solutions with chosen ratios of Cu and Ni by Na_2CO_3 at room temperature under sonification and drying at 80–90°C. They insulated NiCu oxide particles in a NaCl matrix in order to avoid particle agglomeration during thermal processing. The next step was reduction in hydrogen at 300–1000°C. They used an additional thermal treatment in argon, whereas temperatures were varied from 600 to 1000°C to determine the best conditions for the particle synthesis. Polydispersed particles of variable chemical and phase compositions were prepared. They used magnetic separation to improve uniformity of T_c and demagnetization rate. They sonificated the suspension of the particles for 30 min, and they then used the magnetic separation at different temperatures to obtain fractions of the particles with a more uniform T_c. Heating of a 10 mg/ml suspension of the particles with AMF resulted in heating to 43°C, at which the heating stopped, while the initial mixture of the particles continued heating well above this temperature. With this, they demonstrated the potential of magnetic separation for obtaining particles with more uniform thermal demagnetization characteristics. They measured the SAR of the water suspensions of NiCu NPs by heating 1 ml of 10 mg/ ml suspension in a thermally isolated cell in AMF of 440 kHz. A rat-liver cancer model with a working bloodstream was used to test the preparations' effectiveness. Most of the particles accumulated in the capillaries of the rat liver (including the cancer). Applying a magnetic field using a frequency of 440 kHz on the liver resulted in temperature stabilization at 42°C. The particles' acute toxicity was reasonably low [24].

Kwon et al. [46] studied the formation of dispersed powder compositions in order to determine phase formation and redistribution of Cu and Ni atoms between the surface and bulk of the particles during dispersion and cooling of electrical explosion products. They used NiCu alloy wires (6, 12, 23, and 45 wt.% Ni) with a diameter of 0.3 mm, while the explosions were carried out in argon at a pressure of 1.5×10^5 Pa. They vacuumed the experimental setup up to 100–200 Pa, before they filled it. The specific energy input into the wire $W_{(\text{the energy input into the wire})}/W_{s(\text{sublimation energy of the wire})}$ was one of the main parameters that influenced the properties of the produced nanopowder. They prepared powder samples at the same charge voltage with varied content of Ni-Cu alloy components. They settled the powder in a special collector and passivated it in an oxygen-controlled argon atmosphere. SEM analysis (JEOL JSM-840, Japan) confirmed the powder's polydispersity and a spherical particle shape. The consequence of condensation of the gaseous phase on the surface of the liquid droplets and by condensation on nuclei in the gaseous phase was particles of 0.3–1.0 μm in diameter, while the finest formed particles were of 0.1–0.15 μm in diameter. They related the formation of large spherical particles of 1–10 μm in diameter to a so-called end-effect: destruction of the conductor ends at lower current density. They

established that the increase of the specific energy W/W_s input into conductors was accompanied by increase of the powder dispersity and also by increase of the specific surface area [46].

Bahlawane et al. [47] investigated a novel method to produce Ni-based alloys. They used the pulsed-spray evaporation (PSE) chemical vapor deposition (CVD) process in a hydrogen-free atmosphere. Their cold-wall CVD reactor used nitrogen as the carrier gas and ethanol as the reducing agent. Precursors were admitted as a single liquid feedstock in a pulsed way. The frequency in the CVD reactor of 1 Hz and an opening time of 25 ms resulted in a feeding rate of 2.3 ml/min. They dissolved the metal acetylacetonates ($Cu(aca)_2$, $Ni(aca)_2$) with the desired ratios in ethanol to obtain a total metal concentration of 5×10^{-3} mol/l. The reaction temperature of the fcc crystal structure growth in this study was 350°C. The XRD peaks showed a steady shift to low diffraction angles, indicating the insertion of Cu into the lattice of Ni. The analysis of the formed film composition showed that the fraction of Cu in the deposited film increased linearly with its fraction in the liquid feedstock, which enabled the formation of NiCu thin film alloys with a very variable composition. With SEM analysis, they analyzed the morphology of Ni-Cu alloy compositions. They found that the Ni-rich films formed from the less densely packed crystals, which corroborated with the significantly broadened XRD diffraction peaks. A coarser morphology and a heterogeneously distributed particle size of Cu-rich compositions were found. Interestingly, near a Ni/Cu ratio of 1, the films exhibited a structure with the highest apparent density. They prepared and investigated also Ni-Co and Ni-Ag alloys [47].

Pál et al. [48] synthesized Cu, Ni, and NiCu NPs using the solution-combustion method, followed by reduction in hydrogen atmosphere. They dissolved the Ni/Cu nitrate salts (both from Fluka, Germany) (different molar ratios) and citric acid (Fluka, Germany) in distilled water and heated the mixture for 2 h at 60°C in a water bath. They subsequently added EG (Fluka, Germany) to the solution, and then they evaporated the medium at 90°C. After the evaporation process, when gel products were formed, they heated the product in an oven at 150°C for 1 h, which resulted in the formation of voluminous "as-prepared" oxides. They reduced the formed oxides under hydrogen atmosphere at 500°C for 5 h. NiCu alloy characteristic peaks with an fcc crystal structure confirmed the successful preparation (confirmed using a Siemens D500 XRD, Germany). Increasing the Ni content led to particle shape changes (from ellipsoid to irregular) and to a significant increase in particle size with a broad size distribution. They investigated also their applications in aerosol printing for preparation of conductive microstructures [48].

3 Surface modification of magnetic NiCu MNPs

MNPs are often functionalized to improve their potential for biomedical applications [49, 50]. Among the most used materials for coating MNPs, polymer coatings of natural (e.g. dextran and chitosan) and synthetic (e.g. PVP, PEG, and poly(vinyl alcohol)) origin are quite popular [49]. To enhance their water solubility, also other organic molecules (e.g. oleic acid and oleylamine) can be used [51]. But the most common coatings on MNPs are still based on either gold or silica [51]. All abovementioned coating types were already studied in relation to NiCu MNPs.

3.1 PEG surface functionalization

Chatterjee et al. [33] synthesized NiCu alloys through a combined method of polyol reduction and physical melting. The resulting particles were coated with a biodegradable PEG coating using two different methods. In the first, the NiCu particles were suspended in a PEG solution (Sigma-Aldrich, USA), whereas ultrasonification was used to prepare a homogenous dispersion. In the second, an oil (mixture of *n*-hexane, mineral oil, and sodium sesquioleate, all from Sigma-Aldrich, USA) in water (suspension of NiCu particles in a PEG solution) microemulsion was prepared by ultrasonification, followed by cross-linking. After 1 min of ultrasonification, glutaraldehyde was added to the emulsion and stirred for 2 h. TEM analysis (JEOL 2010, Japan) showed a larger tendency toward composite materials for the first method, whereas the second method mostly resulted in encapsulated spherical NiCu particles. The sizes of the encapsulated particles were in the range of 200–500 nm (depending on the pure NiCu particle size). The saturation magnetization (Quantum Design MPMS 5 SQUID magnetometer, USA) for the composition $Ni_{70}Cu_{30}$ was ~6–8 emu/g [33].

Biswas et al. [52] produced a magnetic NiCu nanoalloy exhibiting chain-like structures in the presence of two different polymers. The alloy nanostructures were prepared by reduction of Ni and Cu acetate by hydrazine hydrate in ethanol in the presence of the two polymers [e.g. PEG and poly(4-vinylphenol) (PVPh) (both obtained from Aldrich, USA)] as stabilizing and structure-directing agents,

respectively. The final products were NiCu-PEG and NiCu-PVPh alloy nanostructures. A pure NiCu alloy sample was used for control experiments. The obtained NiCu-PEG alloy sample was easily dispersible in both water and some organic solvents (dioxan, xylene, acetonitrile, and ethanol, all from Merck, India), while the NiCu-PVPh sample was well dispersed in water and in dimethylformamide (DMF) (Merck, India). They explained that the dispersity of these alloy samples in different solvents indicated the presence of respective polymers on the surface of the formed alloy nanostructures. With FTIR analysis (Perkin-Elmer Spectrum 400 spectrometer, USA), they showed bands corresponding to PEG and PVPh polymers. Based on the FTIR data, they claimed that NiCu nanochains were capped with either PVPh or PEG polymer. With magnetic measurements (Quantum Design, MPMS XL, USA), they indicated that these alloy samples were soft ferromagnetics in nature. The saturated magnetization of coated NPs was higher than the value of bare NiCu, which they ascribed to the presence of an oxide layer deposited on the alloy NPs' surface. TEM analysis (JEOL 2010E, Japan) of the NiCu-PEG sample showed the formation of chain-like assembled nanostructures composed of small-sized magnetic alloy nanospheres with an average diameter of 8 ± 1.1 nm. In the case of the NiCu-PVPh sample, the nanochain consisted of spherical alloy particles with a size of 7.5 ± 1.8 nm [52].

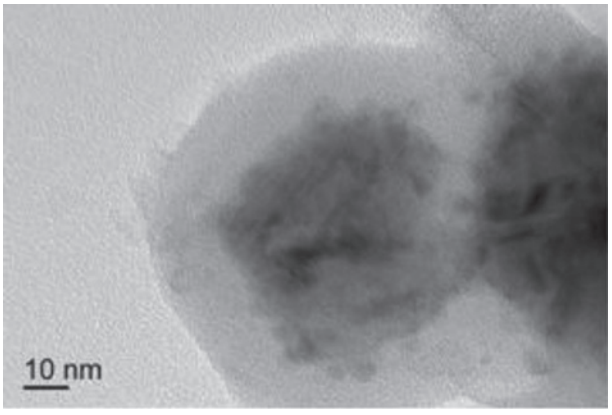

Figure 12: TEM image of magnetic particles with the $Cu_{27.5}Ni_{72.5}$ composition coated with silica. Reproduced with permission from IEEE: *Transactions on Magnetism* [40].

3.2 Silica surface functionalization

Pramanik et al. [53] synthesized NiCu fcc NPs with tunable atomic ratios in SiO_2 films. First, they prepared undoped inorganic-organic hybrid sols using TEOS, 3-(glycidoxypropyl)trimethoxysilane (GLYMO), *n*-butanol, water, methanol, HNO_3 (all obtained from S.D. Fine Chem Limited, India), and aluminum acetylacetonate $(Al(acac)_3$, obtained from Lancaster, UK) [53]. They prepared five different sols for metal ion doping with varying compositions of $Ni_{1-x}Cu_x$ ($x = 0$, 0.333, 0.5, 0.666, 1). The molar ratio of $Ni_{1-x}Cu_x$:$SiO_2 = 20{:}80$ was constant in all the cases. They prepared also the undoped sol with similar equivalent of SiO_2. In the next step, they used silica glass substrates for coating. They dried five different thin-film samples from the $Ni_{1-x}Cu_x$ at 60°C for 1 h and at 90°C for another 1 h, then subjected them to heat treatment in two consecutive steps (at 450°C in air for 1 h to remove the organics followed by heating in a 10 wt.% H_2/90 wt.% Ar atmosphere at 750°C for 1 h to complete the alloy formation). The same preparation method was used for undoped films on polished silicon wafer. Thickness of the films after the final heat treatment was 310 ± 10 nm, while the adherence and abrasion-resistant properties were excellent [53]. XRD (Rigaku SmartLab, Japan) confirmed the presence of an fcc NiCu alloy with a crystallite size of 6 nm. TEM (Tecnai G2 30ST, FEI, USA) image showed an average particle size of 6.35 nm and confirmed the embedded NPs in the silica matrix [53].

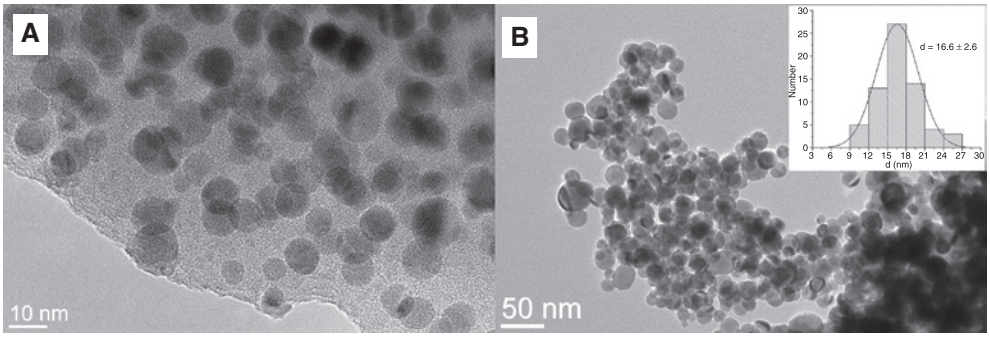

Figure 13: TEM micrographs serve as a good base for size evaluation of prepared particles. (A) Typical TEM images of magnetic particles of sample $Ni_{67.5}Cu_{32.5}$ embedded in a silica matrix and (B) bare alloy particles and the corresponding histogram. Reproduced with permission from Elsevier: *Journal of Alloys and Compounds* [23].

Stergar et al. [40] and Ferk et al. prepared NiCu MNPs using two different synthesis methods, namely, the microemulsion method and the sol–gel method [23, 26]. To prevent agglomeration, they protected MNPs with silica. In the case of the microemulsion method, they synthesized MNPs in a cationic water-in-oil microemulsion based on metal chlorides, hydrazine hydrate, and NaOH [40]. A 10-nm-thick silica layer (measured by TEM, JEOL 2010F, Japan) on the as-prepared NiCu particles was prepared using an alcohol solution of TEOS, PVP as a surfactant, and ultrasonification for 24 h at 60°C. An example is the sample with the composition $Cu_{27.5}Ni_{72.5}$ and a T_c of 65°C on Figure 12 [40].

No significant differences in T_c values were found, and the magnetization of uncoated (as-prepared) and coated MNPs was found. The silica coating prevented agglomeration during thermal treatment and improved the particle biocompatibility [40]. In the other method, Ferk et al. prepared NiCu alloy MNPs in a silica matrix using the sol–gel method [23, 26]. In the first step, they prepared solutions of Ni and Cu salts, citric acid, deionized water, ethanol, and TEOS. They dried the prepared sol for 3 days at room temperature, followed by calcination of the formed gel in air at 500°C for 24 h [26] and at 800°C for 6 h [23]. The result was a powder consisting of Ni and Cu oxides in a SiO_2 matrix. Homogenization was performed in a H_2/Ar atmosphere to obtain the final product of NiCu MNPs in a SiO_2 matrix. NiCu MNPs were extracted from the SiO_2 matrix using an etching solution (mixture of NaOH/hydrazine hydrate) under stirring for 24 h in an Ar atmosphere [23, 26].

When we compare the results of TEM analysis (JEOL 2010F, Japan) of NPs produced by the sol–gel method shown in Figure 13 with the particles produced with other two methods – mechanical milling and microemulsion technique – we can conclude that this method is convenient because it produces particles with a narrow particle size distribution and enables a better control of the T_c. Silica prevented agglomeration of MNPs during thermal treatment, although their magnetic and calorimetric properties were negatively affected. Figure 13 shows typical TEM images (measured by JEOL 2010F, Japan) of MNPs embedded in silica matrix.

3.3 Fatty acids as surface functionalization

Wen et al. [39] synthesized NiCu MNPs and coated them with oleic acid during a microemulsion synthesis. TEM analysis (JEO JEM-1200EX, Japan) showed uniform non-agglomerated particles with an average size of 4–7 nm.

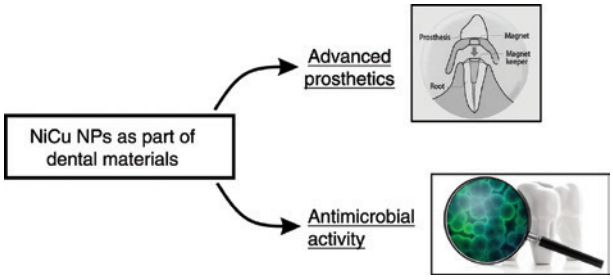

Figure 14: Possible biomedical applications of NiCu MNPs as part of dental materials. Upper right: MNPs can be used as part of prosthetic dental materials, where they can enable advanced mechanical functions or also serve for therapeutic means (targeted delivery). Bottom right: Many different MNP (Ni, Cu, Ag, etc.) based materials have also antimicrobial properties.

The presence of oleic acid (Sinopharm Chemical Reagent Co. Ltd., China) on MNP surface was confirmed using TGA (NETZSCH STA409PC, USA), where a weight loss from 572.2 to 651.9 K corresponded to the evaporation and decomposition of oleic acid. The magnetic properties indicated that the as-prepared amorphous alloy MNPs had unique soft magnetic properties [39].

4 Biomedical applications of magnetic NiCu MNPs

4.1 Development of a ferromagnetic material with adaptable Curie temperature

Among all materials applicable for magnetic hyperthermia in cancer treatment, iron oxides are the most attractive materials because of their high magnetization, biocompatibility, simple synthesis, and relatively high dissipation but with the disadvantage that they possess a relative high Curie point and might overheat the body tissue around the targeted location. The generated heat can be controlled using ferromagnetic NPs with adaptable T_c that can be set to the therapeutic range (42–46°C), as for instance in La-manganates $La_{1-x}Sr_xMnO_3$, Gd-doped iron oxides [54, 55], and $Ni_{1-x}Cu_x$ [22, 23, 26]. In the latter case, the T_c of the final product can be simply controlled through variation of the chemical composition of such materials. This strategy regarding the overheating of the surrounding tissue is very effective since the NPs are autoregulating; i.e. when the T_c is achieved, there will be no heat generated. On the other hand, these NPs must be protected with a biocompatible coating on the bases of silica or noble metals.

The NiCu MNPs are relatively new sustainable nanomaterials appropriate for biomedical applications. As already mentioned above, the interest in their use for biomedical applications is steadily increasing (Figure 2). As the NiCu MNPs can be used for a wide range of biomedical applications, recent findings suggest that these are among the most promising materials especially for multimodal cancer therapies (e.g. combination of MH and controlled drug delivery) [6, 56], as interstitial implants [35, 36], and as part of dental materials [10, 57] (Figure 14).

4.2 State of the art in the field of research to NiCu MNPs

Because of the growing interest in NiCu-based materials for biomedical applications, the following paragraphs summarize their applicability in biomedicine focusing specifically on their properties that render them suitable for such use.

MH is a type of cancer treatment that uses biocompatible MNPs with a controlled T_c (42–46°C) in order to destroy cancerous cells with minimal damage to healthy surrounding tissues and cells [6]. Researchers found that the NiCu MNPs exhibit a tunable T_c in the desired temperature range (equal to the mentioned therapeutic temperature between 42°C and 46°C) and are therefore ideal candidates for use in magnetic hyperthermia [22, 24, 25, 33, 34].

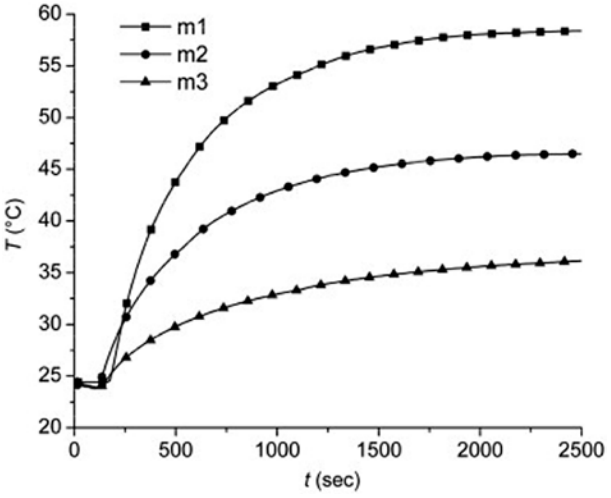

Figure 15: Time dependence of the self-heating temperature on the magnetic field at 104 kHz and the different intensity of the magnetic field for $Cu_{27.5}Ni_{72.5}$. 1-H = 3830 A/m, 2-H = 3130 A/m, and 3-H = 2408 A/m, respectively. Reproduced with permission from Elsevier: *Journal of Magnetism and Magnetic Materials* [22].

Bettge et al. [34] used a simple process that combined melting and ball milling of bulk materials to prepare NiCu alloy particles in the submicron range for possible self-controlled magnetic hyperthermia treatment. The fine ball milled powder had an effective particle diameter of 436 nm with a half-width distribution of 218 nm and showed the desired range of T_c (46–47°C) for self-regulating magnetic hyperthermia. TEM analysis (JEOL 2010, Japan) showed that some particles were spherical and some exhibited a flake-like geometry [34].

Chatterjee et al. [33] synthesized PEG-coated NiCu NPs using the polyol reduction method. The uncoated NPs exhibited a T_c of ~77°C, while the PEG-coated NPs showed a T_c of ~46°C that is within the desired range. The saturation magnetization of NPs was 6–8 emu/g for the encapsulated NPs. Both mentioned results confirmed the potential of these NPs for use in MH treatment of cancer [33].

Kuznetsov et al. [24] synthesized NiCu alloy MNPs by using several techniques. The best results were obtained by using coprecipitation of Cu and Ni salts by Na_2CO_3 at room temperature, followed by reduction in hydrogen at 300–1000°C. Different grinding and separation techniques were used to obtain more uniform particles in size and composition, hence exhibiting a more controllable T_c for use in local magnetic hyperthermia. The resulting NPs were tested on an animal tumor model (rat liver), in which the possible application of NiCu alloy MNPs as mediators for magnetic fluid hyperthermia was demonstrated [24].

Ban et al. [22] prepared NiCu alloy particles in the nanometer range by mechanical milling intended for use in magnetic hyperthermia. They optimized milling conditions, and the result was a nanocrystalline $Ni_{72.5}Cu_{27.5}$ alloy with a crystallite size of around 10 nm and a suitable T_c (45°C) for magnetic hyperthermia. The hysteresis loops of the ball-milled alloy powders showed no remanent magnetization, which is characteristic for superparamagnetic NPs.

Moreover, the $Ni_{72.5}Cu_{27.5}$ sample showed a significant heating effect, indicating that these NiCu alloys might be interesting candidate materials for self-regulating magnetic hyperthermia applications [22]. The magnetic heating effects of the solid powdered samples of $Cu_{27.5}Ni_{72.5}$ with a T_c of 45°C, which is in a medically appropriate range, were measured. The measurements were conducted in a conventionally built system that generates an AMF with a nominal field strength of 2 kA/m and a maximum frequency of 104 kHz. The temperature rise of the calorimeter field with the powdered sample for different magnetic fields is shown in Figure 15 [22].

Stergar et al. [40] synthesized magnetic Ni_xCu_{1-x} NPs using water-in-oil (w/o) microemulsions. TEM analysis

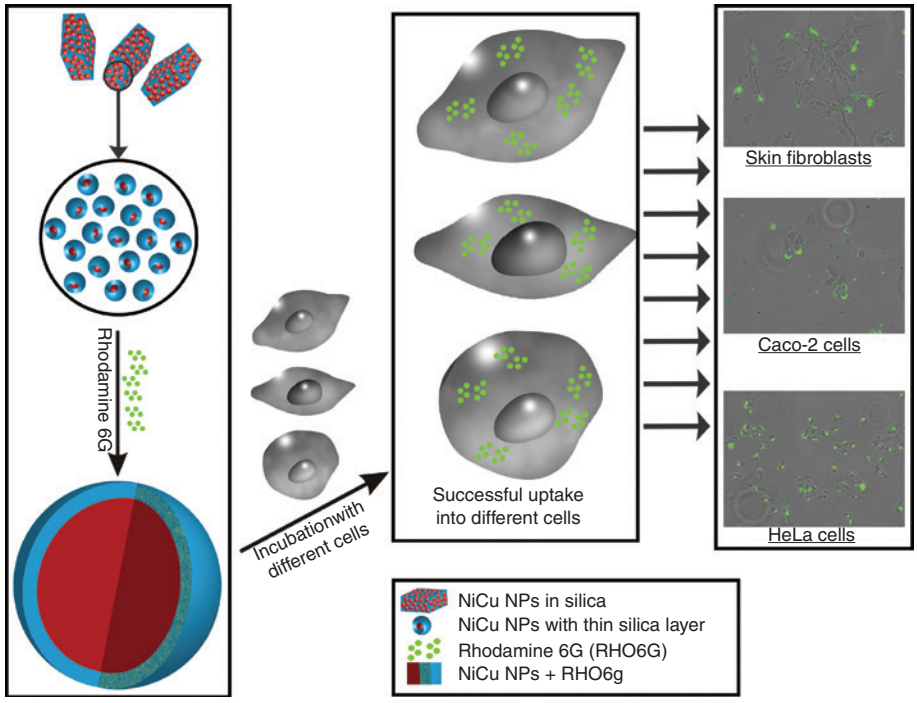

Figure 16: Potential use of NiCu MNPs as an efficient material for a bimodal cancer therapy (simultaneously enabling magnetic hyperthermia and providing the possibility to target and position them as the desired target site). Reproduced with permission from Springer: *Journal of Sol-Gel Science and Technology* [58].

(JEOL 2010F, Japan) showed partially agglomerated NPs with an average size of ~30 nm. The T_c of the as-prepared samples was close to that of pure Ni, indicating a core-shell structure. An additional homogenization step was performed (in a reducing atmosphere in tube furnace at 900°C) to reach a homogenous distribution of Ni and Cu, forming a solid solution with a T_c in accordance with the nominal composition. A silica coating was prepared to avoid NP agglomeration, which did not affect the T_c (~65°C) [40]. Further optimizations had to be required to shift the T_c to the desired therapeutic range.

Ferk et al. [26] synthesized NiCu alloy MNPs with a narrow size distribution by reducing a Ni and Cu-oxide mixture in a silica matrix, obtained with the sol–gel method. The final product was $Ni_{1-x}Cu_x$ MNPs in a SiO_2 matrix. The matrix was removed using etching with NaOH/hydrazine hydrate. Only spherical NPs of $Ni_{67.5}Cu_{32.5}$ with a narrow size distribution remained. The resulting NPs T_c (65°C) was determined using a modified TGA/SDTA method. Ferk et al. [26] were the first who reported the synthesis of superparamagnetic NiCu alloy particles with a narrow particle size distribution and a controlled T_c for use in MH [26].

Amrollahi et al. [25] evaluated the cytotoxicity and magnetic characteristics of $Ni_{0.5}Cu_{0.5}$ NPs synthesized by mechanical milling. With XRD analysis (Philips PW-1730 diffractometer, Belgium), they proved that single-phase $Ni_{0.5}Cu_{0.5}$ NPs have been synthesized after ball milling (30 h) and heat treatment (1 h, 500°C). TEM analysis (Philips CM 300, Belgium) showed a narrow particle size distribution with an average size ~20 nm, although the particles were predominantly agglomerated. The T_c of the single-phase $Ni_{0.5}Cu_{0.5}$ was 44°C. Biocompatibility was proven through proliferation testing using hMSCs. Their research and results showed that single-phase $Ni_{0.5}Cu_{0.5}$ could be a possible candidate for magnetic hyperthermia [25].

Paulus et al. [35] investigated ferromagnetic materials with a low T_c for use as interstitial implants for fractionated hyperthermia treatment of prostatic disease. For this purpose, they used NiCu (Ni/28 wt.% Cu) and palladium-cobalt (Pd/6.15 wt.% Co) alloy samples. They melted both alloys in a carbon arc furnace, and in the next step, they used a recrystallization heat treatment at 1000°C. They spot-welded annealed NiCu and PdCo samples to Cu wire connections and sealed the junction with a water-resistant epoxy adhesive. The remaining surface of the thermal seeds was polished with 1-μm diamond paste to minimize surface contamination. They found that the rates of corrosion estimated by the long-term immersion tests of both alloys were considerably lower than the initial corrosion rates. This difference was explained through formation of

passivation layers. They established that the PdCo alloy exhibited better resistance to corrosion than NiCu, as implied by the lower corrosion potential and faster time to stabilize in solution. Paulus et al. [35] determined that the PdCo alloy exhibited excellent corrosion resistance *in vitro*, an improvement over the previously studied NiCu alloy. The investigated alloys had potential as a long-term implant material for interstitial hyperthermia treatment.

Argueta-Figueroa et al. [57] investigated the antibacterial activity of Cu, Ni, and bimetallic NiCu MNPs for potential use in dentistry. They prepared bimetallic NiCu MNPs by chemical reduction with $NaBH_4$. The antibacterial activity was evaluated on the standard human pathogenic *Staphylococcus aureus* (gram-negative) and *Escherichia coli* (gram-positive), as well as using the dental pathogen *Streptococcus mutans*. In the case of bimetallic NiCu NPs, the XRD analysis (Bruker D8 Advance, Germany) showed three different crystal structures: NiCu, Ni oxide, and Cu (I) oxide. They found that the experimental parameters played an important role in the MNP synthesis. The pH was very important to obtain stoichiometric nanoalloy MNPs, determined by the redox potential of each metal. The obtained MNPs were smaller than 25 nm with a low polydispersity. Cu NPs showed a bactericidal effect against *S. aureus*, *E. coli*, and *S. mutans*, while Ni NPs and bimetallic NiCu NPs exhibited only a bacteriostatic effect on the same microorganisms. Argueta-Figueroa et al. [57] concluded that the evaluated MNPs have promising properties for applications in dentistry.

Recently, Stergar et al. [58] demonstrated a concept to design a novel innovative drug delivery system based on $Ni_{67.5}Cu_{32.5}$ in a silica matrix that can deliver a model fluorescent drug (RHO6G, Sigma-Aldrich, Germany) to various human cells (human fibroblast cell line, HeLa, Caco-2, all obtained from ATCC, UK). Considering the already proven suitable magnetization of such a composition, the authors rightly claim that such a material can provide a dual therapy of cancer. Namely, the prepared materials can induce MH and at the same time act as an efficient delivery system for drugs to the cell interior [58]. Figure 16 shows a schematic depiction of their achievement.

5 Conclusions

In this review, we described different available methods for the preparation of NiCu NPs, their resulting properties, and the already developed methods for their functionalization. The use of magnetic NiCu NPs in biomedical applications is of high interest by different research groups, whereas ours is at the forefront of this research. Expansion of the available subdisciplines of research is inevitable. For example, we are already studying the possible incorporation of NiCu MNPs into wound dressings or similar materials to be used either as topical or transdermal formulation in skin cancer treatment. Magnetic NiCu NPs also possess a high potential to be used as part of multimodal cancer therapies, if they are functionalized and used as magnetically guided carriers for effective antitumor drugs. Such combined treatments have a great future in modern cancer therapies.

Acknowledgment: This work has been financially supported by the Slovenian National Agency (Javna Agencija za Raziskovalno Dejavnost RS, Funder Id: 10.13039/501100004329, grant numbers P3-0036 and J2-6760).

Conflict of interest statement: The authors declare no conflict of interest.

References

[1] Liu Z, Kiessling F, Gätjens J. Advanced nanomaterials in multimodal imaging: design, functionalization, and biomedical applications. *J. Nanomater.* 2010, 2010, 15.
[2] Tartaj P, del Puerto Morales M, Veintemillas-Verdaguer S, González-Carreño T, Serna C. The preparation of magnetic nanoparticles for applications in biomedicine. *J. Phys. D: Appl. Phys.* 2003, 36, R182.
[3] Lu A-H, Salabas EL, Schüth F. Magnetic nanoparticles: synthesis, protection, functionalization, and application. *Angew. Chem., Int. Ed.* 2007, 46, 1222–1244.
[4] Berry CC, Curtis AS. Functionalisation of magnetic nanoparticles for applications in biomedicine. *J. Phys. D: Appl. Phys.* 2003, 36, R198.
[5] Le Trequesser Q, Seznec H, Delville M-H. Functionalized nanomaterials: their use as contrast agents in bioimaging : mono- and multimodal approaches. *Nanotechnol. Rev.* 2013, 2, 125–169.
[6] Kumar CSSR, Mohammad F. Magnetic nanomaterials for hyperthermia-based therapy and controlled drug delivery. *Adv. Drug Delivery Rev.* 2011, 63, 789–808.
[7] Durr S, Janko C, Lyer S, Tripal P, Schwarz M, Zaloga J, Tietze R, Alexiou C. Magnetic nanoparticles for cancer therapy. *Nanotechnol. Rev.* 2013, 2, 395–409.
[8] Schwarz M, Dorfler A, Engelhorn T, Struffert T, Tietze R, Janko C, Tripal P, Cicha I, Durr S, Alexiou C, Lyer S. Imaging modalities using magnetic nanoparticles – overview of the developments in recent years. *Nanotechnol. Rev.* 2013, 2, 381–394.
[9] Gmeiner WH, Ghosh S. Nanotechnology for cancer treatment. *Nanotechnol. Rev.* 2015, 3, 111–122.
[10] Wong J, Prout J, Seifalian A. Magnetic nanoparticles: new perspectives in drug delivery. *Curr. Pharm. Des.* 2017, 23, 2908–2917.

[11] Andra W, Nowak H. *Magnetism in Medicine: A Handbook*. Wiley: New York, 1998.
[12] Häfeli U, Schütt W, Teller J, Zborowski M. *Scientific and Clinical Applications of Magnetic Carrier*. Springer: Berlin, 2013.
[13] Mornet S, Vasseur S, Grasset F, Veverka P, Goglio G, Demourgues S, Portier J, Pollert E, Duguet E. Magnetic nanoparticle design for medical applications. *Prog. Solid State Chem.* 2006, 34, 237–247.
[14] Hergt R, Hiergeist R, Hilger I, Kaiser WA, Lapatnikov Y, Margel S, Richter U. Maghemite nanoparticles with very high AC-losses for application in RF-magnetic hyperthermia. *J. Magn. Magn. Mater.* 2004, 270, 345–357.
[15] Ito A, Matsuoka F, Honda H, Kobayashi T. Antitumor effects of combined therapy of recombinant heat shock protein 70 and hyperthermia using magnetic nanoparticles in an experimental subcutaneous murine melanoma. *Cancer Immunol. Immunother.* 2004, 53, 26–32.
[16] Andrä W, Häfeli U, Hergt R, Misri R. Application of magnetic particles in medicine and biology. In *Handbook of Magnetism and Advanced Magnetic Materials*, Kronmüller H, Parkin S, Eds., John Wiley and Sons: Chichester, 2007, pp. 2536–2568.
[17] Chikazumi S, Graham CD. *Physics of Ferromagnetism*, 2nd ed., Oxford University Press: Oxford, 2009.
[18] Salunkhe AB, Khot VM, Pawar S. Magnetic hyperthermia with magnetic nanoparticles: a status review. *Curr. Top. Med. Chem.* 2014, 14, 572–594.
[19] Laurent S, Forge D, Port M, Roch A, Robic C, Vander Elst L, Muller RN. Magnetic iron oxide nanoparticles: synthesis, stabilization, vectorization, physicochemical characterizations, and biological applications. *Chem. Rev.* 2008, 108, 2064–2110.
[20] Laurent S, Dutz S, Häfeli UO, Mahmoudi M. Magnetic fluid hyperthermia: focus on superparamagnetic iron oxide nanoparticles. *Adv. Colloid Interface Sci.* 2011, 166, 8–23.
[21] Mahmoudi M, Sant S, Wang B, Laurent S, Sen T. Superparamagnetic iron oxide nanoparticles (SPIONs): development, surface modification and applications in chemotherapy. *Adv. Drug Delivery Rev.* 2011, 63, 24–46.
[22] Ban I, Stergar J, Drofenik M, Ferk G, Makovec D. Synthesis of copper–nickel nanoparticles prepared by mechanical milling for use in magnetic hyperthermia. *J. Magn. Magn. Mater.* 2011, 323, 2254–2258.
[23] Ferk G, Stergar J, Makovec D, Hamler A, Jagličić Z, Drofenik M, Ban I. Synthesis and characterization of Ni–Cu alloy nanoparticles with a tunable Curie temperature. *J. Alloys Compd.* 2015, 648, 53–58.
[24] Kuznetsov AA, Leontiev VG, Brukvin VA, Vorozhtsov GN, Kogan BY, Shlyakhtin OA, Yunin AM, Tsybin OI, Kuznetsov OA. Local radiofrequency-induced hyperthermia using CuNi nanoparticles with therapeutically suitable Curie temperature. *J. Magn. Magn. Mater.* 2007, 311, 197–203.
[25] Amrollahi P, Ataie A, Nozari A, Seyedjafari E, Shafiee A. Cytotoxicity evaluation and magnetic characteristics of mechanothermally synthesized CuNi nanoparticles for hyperthermia. *J. Mater. Eng. Perform.* 2015, 24, 1220–1225.
[26] Ferk G, Stergar J, Drofenik M, Makovec D, Hamler A, Jagličić Z, Ban I. The synthesis and characterization of nickel–copper alloy nanoparticles with a narrow size distribution using sol–gel synthesis. *Mater. Lett.* 2014, 124, 39–42.
[27] Songping W, Jing N, Li J, Zhenou Z. Preparation of ultra-fine copper–nickel bimetallic powders with hydrothermal–reduction method. *Mater. Chem. Phys.* 2007, 105, 71–75.
[28] Feng J, Zhang CP. Preparation of Cu–Ni alloy nanocrystallites in water-in-oil microemulsions. *J. Colloid Interface Sci.* 2006, 293, 414–420.
[29] Hergt R, Andra W, d'Ambly CG, Hilger I, Kaiser WA, Richter U, Schmidt HG. Physical limits of hyperthermia using magnetite fine particles. *IEEE Trans. Magn.* 1998, 34, 3745–3754.
[30] Jordan A, Scholz R, Wust P, Fähling H, Roland F. Magnetic fluid hyperthermia (MFH): cancer treatment with AC magnetic field induced excitation of biocompatible superparamagnetic nanoparticles. *J. Magn. Magn. Mater.* 1999, 201, 413–419.
[31] Pankhurst QA, ConnollyJ, Jones SK, Dobson J. Applications of magnetic nanoparticles in biomedicine. *J. Phys. D: Appl. Phys.* 2003, 36, R167.
[32] Andrä W, Nowak H. *Magnetism in Medicine: A Handbook*, 2nd ed., completely rev. and enl. ed., Wiley-VCH: Weinheim, 2007.
[33] Chatterjee J, Bettge M, Haik Y, Jen Chen C. Synthesis and characterization of polymer encapsulated Cu–Ni magnetic nanoparticles for hyperthermia applications. *J. Magn. Magn. Mater.* 2005, 293, 303–309.
[34] Bettge M, Chatterjee J, Haik Y. Physically synthesized Ni-Cu nanoparticles for magnetic hyperthermia. *Biomagn. Res. Technol.* 2004, 2, 4–9.
[35] Paulus JA, Parida GR, Tucker RD, Park JB. Corrosion analysis of NiCu and PdCo thermal seed alloys used as interstitial hyperthermia implants. *Biomaterials* 1997, 18, 1609–1614.
[36] Sue K, Tanaka S, Hiaki T. Synthesis of Ni–Cu particles by hydrogen reduction in hot-compressed water. *Chem. Lett.* 2006, 35, 50–51.
[37] Durivault L, Brylev O, Reyter D, Sarrazin M, Bélanger D, Roué L. Cu–Ni materials prepared by mechanical milling: their properties and electrocatalytic activity towards nitrate reduction in alkaline medium. *J. Alloys Compd.* 2007, 432, 323–332.
[38] Ahmed J, Ramanujachary KV, Lofland SE, Furiato A, Gupta G, Shivaprasad SM, Ganguli AK. Bimetallic Cu–Ni nanoparticles of varying composition ($CuNi_3$, CuNi, Cu_3Ni). *Colloids Surf., A* 2008, 331, 206–212.
[39] Wen M, Liu Q-Y, Wang Y-F, Zhu Y-Z, Wu Q-S. Positive microemulsion synthesis and magnetic property of amorphous multicomponent Co-, Ni- and Cu-based alloy nanoparticles. *Colloids Surf., A* 2008, 318, 238–244.
[40] Stergar S, Ban I, Drofenik M, Ferk G, Makovec D. Synthesis and characterization of silica-coated $Cu_{1-x}Ni_x$ nanoparticles. *IEEE Trans. Magn.* 2012, 48, 1344–1347.
[41] Leontyev V. Magnetic properties of Ni and Ni–Cu nanoparticles. *Phy. Status Solidi (B)* 2013, 250, 103–107.
[42] Bonet F, Grugeon S, Dupont L, Herrera Urbina R, Guéry C, Tarascon JM. Synthesis and characterization of bimetallic Ni–Cu particles. *J. Solid State Chem.* 2003, 172, 111–115.
[43] Carroll KJ, Calvin S, Ekiert TF, Unruh KM, Carpenter KM. Selective nucleation and growth of Cu and Ni core/shell nanoparticles. *Chem. Mater.* 2010, 22, 2175–2177.
[44] Foyet A, Hauser A, Schäfer W. Double template electrochemical deposition and characterization of NiCo and NiCu alloys nanoparticles and nanofilms. *J. Solid State Electrochem.* 2007, 12, 47–55.
[45] Songping W, Li J, Jing N, Zhenou Z, Song L. Preparation of ultra fine copper–nickel bimetallic powders for conductive thick film. *Intermetallics* 2007, 15, 1316–1321.
[46] Kwon YS, An VV, Ilyin AP, Tikhonov DV. Properties of powders produced by electrical explosions of copper–nickel alloy wires. *Mater. Lett.* 2007, 61, 3247–3250.

[47] Bahlawane N, Premkumar PA, Tian Z, Hong X, Qi F, Kohse-Höinghaus K. Nickel and nickel-based nanoalloy thin films from alcohol-assisted chemical vapor deposition. *Chem. Mater.* 2010, 22, 92–100.
[48] Pál E, Kun R, Schulze C, Zöllmer V, Lehmhus D, Bäumer M, Busse M. Composition-dependent sintering behaviour of chemically synthesised CuNi nanoparticles and their application in aerosol printing for preparation of conductive microstructures. *Colloid Polym. Sci.* 2012, 290, 941–952.
[49] Hao R, Xing R, Xu Z, Hou Y, Gao S, Sun S. Synthesis, functionalization, and biomedical applications of multifunctional magnetic nanoparticles. *Adv. Mater.* 2010, 22, 2729–2742.
[50] Bohara RA, Thorat ND, Pawar SH. Role of functionalization: strategies to explore potential nano-bio applications of magnetic nanoparticles. *RSC Adv.* 2016, 6, 43989–44012.
[51] Gupta AK, Gupta M. Synthesis and surface engineering of iron oxide nanoparticles for biomedical applications. *Biomaterials* 2005, 26, 3995–4021.
[52] Biswas M, Saha A, Dule M, Mandal TK. Polymer-assisted chain-like organization of CuNi alloy nanoparticles: solvent-adoptable pseudohomogeneous catalysts for alkyne–azide click reactions with magnetic recyclability. *J. Phys. Chem. C*, 2014, 118, 22156–22165.
[53] Pramanik S, Pal S, Bysakh S, De G. Cu_xNi_{1-x} alloy nanoparticles embedded SiO_2 films: synthesis and structure. *J. Nanopart. Res.* 2010, 13, 321–329.
[54] Thorat ND, Bohara RA, Malgras V, Tofail SA, Ahamad T, Alshehri SM, Wu KC-W, Yamauchi Y. Multimodal superparamagnetic nanoparticles with unusually enhanced specific absorption rate for synergetic cancer therapeutics and magnetic resonance imaging. *ACS Appl. Mater. Interfaces* 2016, 8, 14656–14664.
[55] Thorat ND, Bohara RA, Yadav HM, Tofail SA. Multi-modal MR imaging and magnetic hyperthermia study of Gd doped Fe_3O_4 nanoparticles for integrative cancer therapy. *RSC Adv.* 2016, 6, 94967–94975.
[56] Iglesias GR, Delgado AV, González-Caballero F, Ramos-Tejada MM. Simultaneous hyperthermia and doxorubicin delivery from polymer-coated magnetite nanoparticles. *J. Magn. Magn. Mater.* 2017, 431, 294–296.
[57] Argueta-Figueroa L, Morales-Luckie RA, Scougall-Vilchis RJ, Olea-Mejía OF. Synthesis, characterization and antibacterial activity of copper, nickel and bimetallic Cu–Ni nanoparticles for potential use in dental materials. *Prog. Nat. Sci.: Mater. Int.* 2014, 24, 321–328.
[58] Stergar J, Ban I, Gradišnik L, Maver U. Novel drug delivery system based on NiCu nanoparticles for targeting various cells. *J. Sol-Gel Sci. Technol.* 2017, doi:10.1007/s10971-017-4513-x. https://link.springer.com/article/10.1007/s10971-017-4513-x#citeas.

Bionotes

Irena Ban
Faculty of Chemistry and Chemical Engineering, University of Maribor, Smetanova Ulica 17, SI-2000 Maribor, Slovenia

Irena Ban is an Assistant Professor in the field of general and inorganic chemistry, teaching at the Faculty of Chemistry and Chemical Engineering and Faculty of Medicine, University of Maribor. Her research field focuses on the investigation, synthesis, and characterization of magnetic nanosized materials for biomedical applications and for forward osmosis processes.

Janja Stergar
Faculty of Medicine, Institute of Biomedical Sciences, University of Maribor, Taborska Ulica 8, SI-2000 Maribor, Slovenia, **janja.stergar@um.si**; and Faculty of Chemistry and Chemical Engineering, University of Maribor, Smetanova Ulica 17, SI-2000 Maribor, Slovenia

Janja Stergar is a postdoc sharing her time between the Institute of Biomedical Sciences, Faculty of Medicine, and the Department of Inorganic Chemistry, Faculty of Chemistry and Chemical Engineering, both at the University of Maribor. Her current research focus is on the synthesis and characterization of NiCu magnetic nanoparticles and their use in biomedical applications.

Uroš Maver
Faculty of Medicine, Institute of Biomedical Sciences, University of Maribor, Taborska Ulica 8, SI-2000 Maribor, Slovenia, **uros.maver@um.si**.
http://orcid.org/0000-0002-2237-3786; and Faculty of Medicine, Department of Pharmacology, University of Maribor, Taborska Ulica 8, SI-2000 Maribor, Slovenia

Uroš Maver is an Assistant Professor and institute head at the Faculty of Medicine, University of Maribor. His main research focus includes topics on *in vitro* preclinical models, surface functionalization, drug delivery systems, tissue engineering, and wound healing, as well as molecular resolution microscopy, especially atomic force microscopy in life sciences.